LBL-10210
UC-94a

AQUIFER THERMAL ENERGY STORAGE — A NUMERICAL SIMULATION OF AUBURN UNIVERSITY FIELD EXPERIMENTS

Chin Fu Tsang, Thomas Buscheck,
and Christine Doughty

January 1980

Prepared for the U.S. Department of Energy under Contract W-7405-ENG-48,
and is the result of work within the Seasonal Thermal Energy Storage Program
managed by the Pacific Northwest Laboratory for the
Department of Energy, Division of Thermal and Mechanical Storage Systems.

DISCLAIMER

LBL- 10210

AQUIFER THERMAL ENERGY STORAGE—
A NUMERICAL SIMULATION OF AUBURN UNIVERSITY FIELD EXPERIMENTS

Chin Fu Tsang, Thomas Buscheck and Christine Doughty

Lawrence Berkeley Laboratory
University of California
Berkeley, California 94720

January 1980

Work performed under the auspices of the U.S. Department of Energy.

This paper is the result of work within the Seasonal Thermal Energy Storage Program managed by the Pacific Northwest Laboratory for the Department of Energy, Division of Thermal and Mechanical Storage Systems.

Abstract

This paper describes the computer simulation of two cycles of a seasonal aquifer thermal energy storage experiment recently carried out by Auburn University. The simulated production temperatures and energy recovery factors agree very well with the field data. A general description of the experiments and the numerical model used are given. Discussions are also given on the determination and choice of various parameters used in the simulations. These are followed by a detailed comparison of simulated and observed temperature distributions.

AQUIFER THERMAL ENERGY STORAGE
A NUMERICAL SIMULATION OF AUBURN UNIVERSITY FIELD EXPERIMENTS

Chin Fu Tsang, Thomas Buscheck and Christine Doughty
Lawrence Berkeley Laboratory
University of California
Berkeley, California 94720

Introduction

For many years confined aquifers have been used for storing fresh water, oil products, and gas, as well as for the disposal of liquid wastes. A vast literature has resulted, primarily dealing with well hydraulics in isothermal systems (Esmail and Kimbler, 1967; Katz and Tek, 1970; Kimbler, 1970; Kumar and Kimbler, 1970; Moulder, 1970; Kazmann, 1971, 1974; Kazmann, Kimbler, and Whitehead, 1974; Smith and Hanor, 1975). However, the concept of storing hot water in aquifers for later use was suggested by several authors only about ten years ago (e.g., Rabbimov, Umarov and Zakhidov, 1971; Meyer and Todd, 1973). Various generic and feasibility studies have since been made (Hausz and Meyer, 1975; Warman, Molz and Jones, 1976; Tsang, Lippmann, Goranson and Witherspoon, 1977; Larson, 1976; Papadopulos and Larson, 1978; Molz, 1978; Tsang, Buscheck, Mangold and Lippmann, 1978; and others). These mostly considered storage of low or moderate temperature water; several focused on economic and institutional considerations as well. The year 1978 saw the first International Aquifer Thermal Energy Storage (ATES) Workshop, held at the Lawrence Berkeley Laboratory (Proceedings, 1978). Current aquifer thermal storage projects are summarized in a periodic Newsletter (ATES Newsletter, 1978, 1979) and two recent review articles (Tsang, 1979; and Tsang, Hopkins and Hellstrom, 1980).

Knowledge gained in previous studies of aquifer storage problems is applicable primarily to isothermal conditions. A successful study of the viability of the ATES concept depends on the development of an adequate understanding of heat, mass, and momentum transport processes under non-isothermal conditions within an aquifer/aquitard system during injection, storage, and production cycles. Because these processes are highly coupled, understanding is most readily achieved using numerical models. Field experiments must also be carried out to measure heat and fluid flow patterns and to detect practical problems.

In 1976 Auburn University completed a first set of field experiments storing cooling water from a steam power plant (Molz et al., 1978). The experiments were analyzed in a numerical simulation study by Papadopulos and Larson (1978), who employed a finite difference model developed for the U.S. Geological Survey (U.S.G.S.) by INTERCOMP (1976). Molz et al. (1979) subsequently completed a second set of field experiments, which included two injection/storage/production cycles. From difficulties experienced in their first experiment, Molz et al. were able to improve significantly on their experimental techniques, thereby achieving a substantial increase in the net quantity of hot water injected into the storage aquifer during both cycles.

This report describes the numerical simulation of the second set of Auburn University field experiments. The simulation was carried out at the Lawrence Berkeley Laboratory (LBL) using three-dimensional models developed at LBL over the past several years. The next section of this report is a brief description of the two injection/storage/production cycles, followed

by a qualitative description of the semi-analytic model used to evaluate hydraulic parameters and of the numerical model used to simulate the experiment. The following section describes (1) the determination of the hydraulic and thermal parameters, (2) the design of the various computer meshes used in the simulation, (3) the simulation of the injection and production-rate histories, and (4) the rationale behind various simplifications that were made in carrying out the simulation. This is followed by a detailed comparison of the simulated thermal field with the experimental data. The report concludes with a summary and some general remarks.

The Experiments

Details of the experiments recently performed by the Water Resources Research Institute of Auburn University are described in a companion paper by Molz, Parr and Anderson. The test facility and well field shown in Figure 1 were constructed on land provided by the Alabama Power Company in northeastern Mobile County, Alabama. The injection/production well was screened in the upper half of a uniform confined aquifer, approximately 21 m thick. The aquifer matrix consists primarily of medium to fine sand, with approximately 15 weight percent interstitial silt and clay. The aquifer occurs from about 40 m to 61 m below the land surface and is capped by a 9 m thick clay sequence; it is bounded below by another clay sequence of undetermined thickness. Above the upper clay unit lies another aquifer, which provided the injection water.

The first six-month injection/storage/production cycle involved the injection and recovery of about 55,000 m^3 of water, heated to an average temperature of 55.2°C. The ambient water temperature of the supply and storage aquifers was 20°C. After 79.2 days of injection at an average flow rate of 7.89 kg/sec (125 gpm), the warm water was stored for 52.5 days and then pumped out at an average flow rate of 15.65 kg/sec (245.6 gpm) until the temperature of the recovered water fell to 32.8°C. By that time, 66% of the injected energy had been recovered. The injection, storage, and production periods were 1900, 1213, and 987 hours, respectively.

The second six-month cycle was carried out in essentially the same manner as the first. About 58,000 m^3 of water, heated to an average temperature of 55.4°C. was injected, stored for 62.5 days, and then produced. By the time the production temperature had fallen to 32.8°C, 76% of the energy injected during the second injection period had been recovered; the total volume recovered was 67,000 m^3. For the second cycle, the injection, storage, and recovery periods were 1521, 1502, and 1328 hours, respectively.

Description of Models

The first stage of the simulation study involved the determination of the hydraulic parameters of the aquifer---the transmissivity, T, storativity, S, and the location and type (barrier or leaky) of a linear hydrologic boundary---through well test analysis. Conventional type-curve analysis techniques require constant flow rates. To get around this limitation, LBL has recently developed a computer-assisted well test analysis method, program "ANALYZE" (Tsang et al., 1977; McEdwards, 1979), that accounts for the variable flow rates of several production or injection wells.

Briefly, the computational basis of ANALYZE is a least squares minimization routine that uses parameters T, S, and the angle and distance to a hydrologic boundary to calculate the pressure change at locations and times corresponding to observed pressure data. It then adjusts the values of the parameters so that the difference between calculated and observed pressure changes is a minimum. The set of parameters associated with the minimum is then accepted as representative of the aquifer and well system. Further details are described by Doughty, McEdwards, and Tsang (1979).

Once the hydraulic parameters were determined, all of the numerical simulation was carried out using the model "CCC," which stands for conduction, convection, and consolidation. This program was developed at LBL (Lippmann, Tsang and Witherspoon, 1977) to simulate heat and momentum transport in one-, two-, or three-dimensional heterogeneous, anisotropic, nonisothermal porous systems. If required it can also compute the vertical deformation of the porous matrix using the one-dimensional consolidation theory of Terzaghi. This program is based on the so-called Integrated Finite Difference Method; it uses an explicit-implicit iterative procedure to advance in time. Details of the algorithms are given by Edwards (1972); Sorey (1976); Narasimhan and Witherspoon (1976); and Lippmann, Tsang, and Witherspoon (1977). The following properties and physical effects are simultaneously considered in the calculations: (a) the temperature dependence of the heat capacity, viscosity, and density of the fluid; (b) heat convection and conduction in the aquifer/aquitard system; (c) heterogeneity of the aquifer properties; (d) anisotropy of permeability and effective thermal conductivity; (e) regional groundwater

flow; (f) presence of hydrologic barriers; and (g) gravitational effects.

Parameters Used and Mesh Design

As discussed in detail by Doughty et al. (1979), ANALYZE was used to analyze multi-well pressure data from a 36-hour pumping test as well as from the entire injection period of the first Auburn experiment. Results for radial transmissivity and storativity, as well as distance and orientation of the closest barrier, were thus obtained (Table 1). The transmissivity, storativity, and distance values confirm earlier results obtained by the U.S.G.S. (Papadopulos and Larson, 1978).

A linear barrier was located approximately 300 meters away from the injection well at an angle of 315° counterclockwise from a line joining well 7 to well 14 (i.e., lying to the NW of the well field). Since, as shown later, the radius of the hot water storage region in the aquifer extends only 45 m from the injection well, a barrier 300 m away should have had only a small effect and was neglected in the smulation. Possible minor effects of the barrier are noted in the next section.

Molz et al. (1978), also tried to determine the regional groundwater gradient. Although differences in pressure head were close to instrument error, their measurements indicated that the groundwater gradient should be less than 2.96×10^{-4} m/m in the northeast direction. The orientation of the barrier NW of the well field is also northeasterly, consistent with the direction of the regional flow. A groundwater gradient of 2.96×10^{-4} m/m, together with a porosity of 0.25 and transmissivity values as given in Table 1, yields a pore velocity of 0.052 m/day. After the first cycle

injection and storage periods of approximately 130 days, the injected water would have been displaced 6.8 meters relative to the well, but the hot water region would have been displaced only 2.9 meters. In comparison with the radius of the thermal region (~ 45 m), this displacement was thought not to be significant. Thus idealizations were made to represent the storage aquifer as an axisymmetric aquifer/aquitard/well system of effectively infinite areal extent.

The remaining hydraulic parameter values necessary for the simulation could not be obtained directly from the well test analysis: vertical aquifer permeability, k_v, radial and vertical aquitard permeability, k_r^t and k_v^t; and aquitard storativity, S^t. Because the aquitard is a moderately stiff clay and the earlier experiment showed no pressure response in the upper aquifer during injection (until the aquitard ruptured), the aquitard was considered to be relatively impermeable. The hydrologic literature indicates that a permeability ratio of 10^5 between aquifer and aquitard is representative of shallow alluvial clay/sand sequences. A parametric study (Buscheck, Doughty, and Tsang, 1980) has since shown the thermal response in the aquifer to be relatively insensitive to variations of a factor of 10 in this parameter. The literature also indicates that setting the storativity value in the aquitard equal to that in the aquifer is reasonable.

The other major hydrologic parameter to be determined, the radial to vertical permeability ratio, also had to be inferred from experience in the hydrologic literature and from indirect geologic evidence. For the purposes of their study, Papadopulos and Larson (1978) used $k_r/k_v = 10$. This value was also used in the present study. A later parametric study (Buscheck et al., 1980) showed this to be a very critical parameter, with $k_r/k_v = 10$ giving the closest correspondence between the simulated and observed

temperature fields. This value was also used for the permeability ratio in the aquitards, but, as with the magnitude of kr^t, this is felt to be a less critical parameter with regard to the thermal field.

The thermal conductivity of the aquifer and upper aquitard were taken from laboratory values and are listed in Table 2. The porosity of the aquifer and aquitard were assumed to be 0.25 and 0.15, respectively. A recent communication with Fred Molz has indicted that .35 is a better value for aquitard porosity than is .15; a parameter study (Buscheck et al., 1980) has shown that the use of .15 rather than .35 for the aquitard porosity has a negligible effect on the thermal field. The density, heat capacity, and viscosity of the fluid were varied as functions of temperature by interpolating from values given in Table 3, which were taken from Kappelmeyer and Haerel (1974) and Helgeson and Kirkham (1974).

The numerical simulation of the first and second cycles used the mesh shown in Figure 2. The well is positioned at zero radial distance, the mesh having radial symmetry about that axis. In pressure calculations, mesh elements can be increased in size with increasing radius without significantly affecting the accuracy of the results. However, for heat flow calculations within the region of thermal influence ($r \sim 80$ m in the present case), the mesh elements should decrease in size with increasing radius, since for equal time steps the injected hot water will move a smaller radial distance (assuming a constant injection flow rate). In our calculations we compromise by using a mesh with equal radial distance steps within the zone of thermal influence. Outside of this zone, mesh elements can increase in size out to a radial distance of 20 kilometers. This large mesh size makes the system effectively infinite in areal extent (i.e., provides a constant head boundary).

Because fence diagrams (Molz et al., 1978) indicated approximately uniform, horizontal aquifer and aquitard layers, it was possible to model all

horizontal boundaries as having constant elevations. Note the vertical spacing of element in Figure 2. Within the aquifer, the finest resolution was provided near the top and along the elevation interval of the well screen so that the region of greatest thermal influence would have sufficient resolution to simulate buoyancy effects. Very fine vertical spacing was also provided on the aquitard side of the aquitard/aquifer boundary, because in this region the magnitude of heat flow is governed by conduction. Thus, this important process would not be underestimated. Based on experimental data, the upper storage aquifer was considered to be a constant temperature and constant pressure layer and was modeled as one large element.

In order to investigate the effects of numerical dispersion, two additional meshes were employed. While their vertical dimensions were identical to those in the primary or "medium" mesh, the radial spacing of elements within the region of thermal influence were one-half and twice that of the medium mesh. The entire first cycle was simulated using the coarse mesh. However, only the injection period of the first cycle was simulated using the fine mesh because of the large computer cost involved. Results are presented in the next section.

In the simulation of the first cycle on the medium mesh, the execution of flow cycles (i.e., solution of the pressure equation) required a tremendous number of very short time steps for numerical stability, leading to prohibitive computer costs. The solution of the pressure equation is related to transient flow effects and is controlled by the storativity parameter. Increasing the storativity while keeping the porosity constant reduces transient effects and thus cut down on computation time. A parameter study (Buscheck et al., 1980) shows that within certain limits, an increase of storativity, while cutting

down on computer time drastically, does not affect the temperature field noticeably. A case was run with a simplified mesh (single layer, regular radial steps) corresponding to Auburn field properties. Several storativity values were used and aquifer temperature profiles, production temperatures, and recovery ratios calculated for each. Selected results (Table 4) show that increasing the storativity by a factor of 20 does not affect temperature fields. Hence, for our simulation, we multiplied the storativity by 20 to save computer cost.

Because neither the flow rate nor the injection temperature were maintained constant during the course of the experiment, for simulation we broke up injection and production periods into many time intervals having averaged values of flow rate (and temperature, for injection periods); mass and energy were conserved for each time interval. Figure 3 shows the experimental and averaged values during the first injection period.

Results of Simulations: First Cycle

Figure 4 shows the simulated temperature contours after only 287 hours, when the effects of buoyancy flow are just becoming evident. By the end of the injection period (1900 hours), the effects of buoyancy flow are apparent and the thermal disturbance has spread to a radial distance of ~ 45 m (Figure 5). Figures 6 through 9 compare the simulated temperature-time dependence with the observed behavior in various wells. While the overall correspondence is good, there is a trend for underprediction of temperatures for early time and overprediction for later time. The transition from underprediction to overprediction occurs when the point of inflection of the thermal front crosses the observation point in question. This shows that the actual thermal front was more smeared than the predicted front, a result of

neglecting the effects of fingering of the thermal front. Another trend within the observed data is that wells to the SE of the injection point showed an earlier temperature response than those to the NW. This reflects the rather modest influence of the barrier that was detected in the well test analysis.

Figures 10 through 12 compare the observed and simulated radial temperature distribution for three depths (measured from the top of the aquifer) at the end of the injection period, t = 1900 hours. These figures provide a different display of the temperature field shown in Figure 5. One should be cautious not to attribute too much significance to all discrepancies between observed and simulated values, since the observed data were taken from all around the well field. Therefore, differences may reflect local inhomogeneities which cause the real system to deviate from the ideal axisymmetric system. Generally, for upper elevations, there is a good correspondence, with a slight underestimation of the smearing of the thermal front. There is a tendency to overpredict temperatures at lower elevations. This suggests a slight underprediction of anisotropy, which in the simulation would allow more hot water to be convected to elevations below the bottom of the well screen during injection.

Figure 13 compares the observed and simulated temperature distributions at the end of the storage period, t = 3113 hours. The effects of buoyancy flow and temperature front smearing are quite evident and heat has penetrated far into the upper aquitard.

Figure 14, the temperature contour plot at the end of the production period, t = 4100 hours, shows a remarkably good correspondence between the observed and simulated temperature fields. This reflects "compensating" processes that tend tend to cancel each other out at the end of an injection/production cycle. Local inhomogeneities (not accounted for in the simulation)

of a relatively high permeability, for example, provide local conduits of greater heat convection away from the well during injection. These same regions, because they contain hotter, less viscous water and because they are areas of relatively high intrinsic conductance for heat convection, also conduct more water towards the well during production. Thus, these processes tend to cancel out upon the completion of an injection/production cycle. The net effect for this case is that the observed temperature field at the end of the injection/production cycle looks very much like the ideal axisymmetric, homogeneous case.

Figure 15, a plot of production temperature versus time, shows remarkably close correspondence between the observed and simulated behavior. Throughout the production period, there is consistently a very slight overprediction ($< 1.0^{\circ}C$), but the curvature of the two curves is very close. This close correspondence reflects the "compensating" processes discussed above. During production, because of the mixing of water drawn in from different elevations, vertical variation of the temperature is also smoothed out. Thus, production temperatures provide only an integrated or lumped picture of what is occurring in the aquifer. As expected, the recovery ratio ($\varepsilon \equiv$ net energy produced/net energy injected for that cycle) is overpredicted by only a modest amount: $\varepsilon_{sim} = 0.68$ versus $\varepsilon_{obs} = 0.66$. This very good correspondence suggests that the simplifying assumptions made in the model simulation were reasonable. It also seems to indicate that a good choice was made for anisotropy. For the field study completed in 1976, Papadopulos and Larsen (1978) predicted an energy recovery ratio of 0.75, whereas the actual value was 0.69. The error in the predicted value may have reflected various experimental difficulties (Molz et al., 1978).

To establish the mesh-independence of our results, we performed these calculations again for a coarser and a finer mesh, the original mesh being

designated as the medium mesh. These mesh designs are discussed in the previous section. Figure 16 compares the radial temperature distribution for the coarse, medium, and fine meshes. As expected, the coarse mesh yields a more smeared front due to numerical dispersion. However, the medium and fine meshes show very little difference. This indicates that, for meshes at least as fine as the primary or medium mesh, heat flow calculations should be effectively mesh-independent. Since all results presented utilized the medium mesh, the effects of numerical dispersion can be considered to be insignificant. It also appears that even the coarse mesh could be relied upon to give satisfactory results.

Figure 17 is the plot of production temperature versus time for the simulation performed with the medium and coarse meshes. A comparison of Figures 15 and 17 shows that for the coarse mesh, there is even a closer correspondence with the observed values than there was for the medium mesh. Consequently, the recovery factor predicted by the coarse mesh is also closer to the observed value, $\varepsilon_{sim} = 0.67$ versus $\varepsilon_{obs} = 0.66$. The coarse mesh consistently predicted slightly lower production temperatures than the medium mesh did, possibly simulating thermal dispersive effects with increased numerical dispersion. The simulation of the fluctuations in actual production using average production rates appears to be reasonable, since the slope changes in the actual production temperature curve are quite closely imitated by the simulated curve.

Results of Simulations: Second Cycle

Although there are relatively few field data from the second cycle, the relation between the simulated and observed behaviors is much like that of the first cycle. Figure 18 shows the temperature contour plot at the end

at the end of injection. The correspondence between the observed data and simulated temperature contours is reasonably good. Note that the isotherms extended farther because heat (representing 18% of the energy injected during the first cycle was left in the aquifer at the end of the first cycle. Most of this residual hot water floated to the top of the aquifer (Figure 14). At the start of the second injection period, the injected hot water tended to flow toward the top of the aquifer because the relatively hot, less viscous water there presented less resistance to flow relative to the rest of the aquifer. Consequently, there was an even greater tendency for hot water to segregate at the top of the aquifer during the second cycle. Figure 18 illustrates this effect. Note also that the thermal front was more diffuse, because the effects of the second injection period were superposed on a temperature distribution that was already smeared at the beginning of the second cycle. Figure 19, the temperature contour plot at the end of the second cycle, shows, again, very good correspondence between the observed and simulated temperature fields. This reflects the same reasons given for the close correspondence at the end of the first cycle.

Figure 20, the production temperature versus time, shows good correspondence with experimental values. For the second cycle, as in the case of the first cycle, the predicted recovery factor is also slightly higher than the observed: $\varepsilon_{sim} = 0.78$ versus $\varepsilon_{obs} = 0.76$. For the two cycles combined, the net recovery factor is $\varepsilon_{sim\ net} = 0.73$ versus $\varepsilon_{obs\ net} = 0.71$. Table 5 lists the energy balances for both cycles. It is apparent that, were the experiment continued, the recovery factor would continue to improve for subsequent cycles.

Conclusion

The first two cycles of a recent series of Auburn University field experiments were simulated and studied. The simulated production temperatures and energy recovery ratio agree very well with field data. This strongly indicates the validity of the numerical model and simulation procedures used, and gives us confidence in predicting performance of future cycles. Larger discrepancies between calculations and experimental data are noticed in detailed temperature distribution comparisons. There appears to be a smoothing and "compensation" effect by which some discrepancies are averaged out and some cancel themselves during the injection-and-production process, so that the final production temperatures are simulated very well. Plans are under way to make predictions for new experiments involving higher storage temperatures and doublet injection-production wells. Calculations are also being initiated to study parameter sensitivity of these results.

Acknowledgments

The cooperation of Fred Molz and David Parr of Auburn University in supplying LBL with their experimental results and in exchanging ideas is appreciated. Discussions with Dr. Marcelo J. Lippmann, Professor Paul Witherspoon, Donald Mangold, Goran Hellstrom and Deborah Hopkins are gratefully acknowledged. Work is supported by Energy Storage Division of the United States Department of Energy (through Oak Ridge National Laboratory and Pacific Northwest Laboratory) under Contract Number W-7405-ENG-48.

References

Aquifer Thermal Energy Storage (ATES) Newsletter, 1978-1979, Chin Fu Tsang, Editor, published by Lawrence Berkeley Laboratory, Berkeley, California 94720, U.S.A.

Buscheck, T., Doughty, C., and Tsang, C.F., 1980, "Aquifer Thermal Energy Storage - Parameter Study" (in progress).

Doughty, C., McEdwards, D., Tsang, C.F., Multiple well variable rate well test analysis of data from the Auburn University Thermal Energy Storage Experiment, LBL Report No. 10194.

Edwards, A.L., TRUMP: A Computer Program for Transient and Steady State Temperature Distribution in Multidimensional Systems," Lawrence Livermore Laboratory, Rpt. UCRL-14754, Rev. 3., 259 p., 1972.

Esmail, O.J., and Kimbler, O.K., 1967, Investigation of the Technical Feasibility of Storing Fresh Water in Saline Aquifers, Water Resources Res. 3: pp. 683-695.

Helgeson, H.C., and Kirkham, D.H., "Theoretical Prediction of the Thermodynamic Behavior of Aqueous Electrolytes at High Pressures and Temperatures: 1. Summary of the Thermodynamics/Electrostatic Properties of the Solvent," American Journal of Science, Vol. 274, pp. 1089-1198, 1974.

INTERCOMP Resources Development and Engineering Inc., 1976, A model for calculating effects of liquid waste disposal in deep saline aquifers. U.S. Geol. Survey Water Resources Inv. 76-61.

Kappelmeyer, O., and Haenel, R., "Geothermics with Special Reference to Applications," Geoexploration Monographs, Series 1, No. 4, Berlin-Stuttgart: Geopublication Associates, Gebruder Borntraeger, 1974.

Katz, D.L., and Tek, M.R., 1970, Storage of Natural Gas in Saline Aquifers, Water Resources Res. 6: pp., 1515-1521.

Kazmann, R.G., 1971, Exotic Uses of Aquifers, Journal Irrig. Drain. Div. ASCE, 97: pp. 515-522.

Kazmann, R.G., Kimbler, O.K., and Whitehead, W.R., 1974, Management of Waste Fluids in Salaquifers, Journal Irrig. Drain. Div., ASCE, 100, pp. 413-424.

Kimbler, O.K., 1970, Fluid Model Studies of the storage of Freshwater in Saline Aquifers, Water Resources Res. 6: pp. 1522-1527.

Kumar, A., and Kimbler, O.K., 1970, Effect of Dispersion, Gravitational Segregation, and Formation Stratification on the Recovery of Freshwater Stored in Saline Aquifers, Water Resources Res. 6, pp. 1689-1700.

Larson, S.P., Papadopulos, S.S., and Mercer, J.W., 1976, Transport of water and heat in an aquifer used for hot water storage: digital simulation of field results, Symposium on uses of aquifer systems for cyclic storage of water, Fall annual meeting of the American Geophysical Union, San Francisco, California, December 9, 1976.

Lippmann, M.J., Tsang, C.F., and Witherspoon, P.A., Analysis of the response of geothermal reservoirs under injection and production procedures, SPE 6537.

McEdwards, D., 1979, Multiwell variable rate well test analysis, Ph.D. thesis, University of California, Berkeley, Lawrence Berkeley Laboratory, Berkeley, California, LBL-9549.

Meyer, C.F., and Hausz, W., 1975, A new concept in electric generation and energy storage, presented at Frontiers of Power Tech. Conf., Oklahoma State University, Stillwater, Oklahoma, October 1-2, 1975.

Meyer, C.F., and Todd., D.K., 1973, Heat storage wells, Water Well Journal, v. 27, no. 10, pp. 35-41.

Molz, F.J., Parr, A.D., and Andersen, F.P., Thermal energy storage in a confined aquifer--second cycle, Journal of Water Resources Research, in press.

Molz, F.J., Parr, A.D., Andersen, P.F., Lucido, V.C., and Warman, J.C., 1979, Thermal energy storage in confined aquifers, Water Resources Research Institute, Auburn University, Auburn, Alabama (preprint), 29 p.

Molz, F.J., and Warman, J.C., 1978, Confined aquifer experiment---heat storage, Proceedings of Thermal Energy Storage in Aquifers Workshop, May 10-12, 1978, Lawrence Berkeley Laboratory, Berkeley, California (Chin Fu Tsang, editor), pp. 46-50.

Molz, F.J., Warman, J.C., and Jones, T.E., 1978, Aquifer storage of heated water: part I---a field experiment, Ground Water, v. 16, no. 4, pp. 234-241.

Moulder, E.A., 1970, Freshwater Bubbles: A Possibility for Using Saline Aquifers to Store Water, Water Resources Res., 6, pp. 1528-1531.

Narasimhan, T.N., and Witherspoon, P.A., "An Integrated Finite Difference Method for Analyzing Fluid Flow in Porous Media," Water Resour. Res., 12, No. 1, p. 57-64, 1976.

Papadopulos, S.S., and Larson, S.P., 1978, Aquifer storage of heated water: Part II---Numerical simulation of field results, Ground Water, v. 16, no. 4, pp. 242-248.

Proceedings of Thermal Energy Storage in Aquifers Workshop, May 10-12, 1978, Lawrence Berkeley Laboratory, Berkeley, California, 94720, U.S.A., Request for copies of the proceedings should be directed to the workshop chairman: Dr. Chin Fu Tsang, Earth Sciences Division, Lawrence Berkeley Laboratory, University of California, Berkeley, California, 94720.

Rabbimov, R.T., Umarov, G.Y., and Zakhidov, R.S., 1971, Storage of solar energy in sandy-gravel ground, Geolliteknika, v. 7, no. 5, pp. 57-64.

Smith, C.G., and Hanor, J.1S., 1975, Underground Storage of Treated Water: A Field Test, Ground Water, 13, pp. 410-417.

References (cont'd.)

Sorey, M.L., "Numerical Modeling of Liquid Geothermal Systems," Ph.D. Thesis, University of California, Berkeley, 65 p., 1975.

Tsang, C.F., 1979, A summary of current studies in aquifer thermal energy storage, Presented at the Second International Helioscience Institute Conference on Alternative Energy, Palm Springs, California, April 8-11, 1978, (LBL-7066).

Tsang, C.F., Buschek, T., Mangold, D., and Lippmann, M., 1979, Mathematical modeling of thermal energy storage in aquifers, Proceedings of Thermal Energy Storage in Aquifers Workshop, May 10-12, 1978, Lawrence Berkeley Laboratory, Berkeley, California (Chin Fu Tsang, editor), pp. 37-45.

Tsang, C.F., Hopkins, D., and Hellstrom, G., 1980, A Review of Current Aquifer Thermal Energy Storage Programs (in preparation).

Tsang, C.F., Lippmann, M.J., Goranson, C.B., and Witherspoon, P.A., 1977, Numerical modeling of cyclic storage of hot water in aquifers, presented AGU Fall Meeting, San Francisco, California, December 6-10, 1976 (LBL-5929).

Tsang, C.F., McEdwards, D., Narasimhan, T.N., and Witherspoon, P.A., Variable flow well test analysis by a computer assisted matching procedure, Paper No. SPE-6547, 47th Annual California Regional Meeting of SPE of AIME, Bakersfield, California, April 13-15, 1977.

Warman, J.C., Molz, F.J., and Jones, T.E., 1976, Step beyond theory---aquifer storage of energy, Proceedings Second Southeastern Conference on Application of Solar Energy (CONF-769423), NTIS.

Table 1.

WELL TEST ANALYSIS RESULTS

$T = 1.05 \times 10^{-2} - 1.14 \times 10^{-2}$ m^2/S

$S = 4.6 \times 10^{-4} - 4.8 \times 10^{-4}$

ANGLE = 315^o

DIST = 305 - 337 m

DIST is the distance from well 1 to the nearest barrier boundary.

ANGLE indicates location of the barrier measured clockwise with reference to a line joining well 7 to well 14.

A transmissivity of 1.09×10^{-2} m^2/sec, an aquifer thickness of 21 m, and a fluid viscosity of .001 Pa-sec yields an aquifer radial permeability of $k_r = 5.3 \times 10^{-11} m^2$.

Table 2.

ROCK PROPERTIES

Aquifer

Specific Heat = 696 $\frac{\text{Joules}}{\text{kg } ^{o}C}$

Thermal Conductivity = 2.29 $\frac{\text{Joules}}{\text{m sec } ^{o}C}$

Density = 2.6×10^{3} kg/m^{3}

Aquitard

Specific Heat = 696 $\frac{\text{Joules}}{\text{kg } ^{o}C}$

Thermal Conductivity = 2.56 $\frac{\text{Joules}}{\text{m sec } ^{o}C}$

Density = 2.6×10^{3} kg/m^{3}

Table 3.

FLUID PROPERTIES

Viscosity

Temperature (°C)	Viscosity (Pa sec)
20	$.1005 \times 10^{-2}$
50	$.545 \times 10^{-3}$
100	$.280 \times 10^{-3}$
150	$.182 \times 10^{-3}$
200	$.135 \times 10^{-3}$

Specific Heat

Temperature (°C)	Specific Heat $\left(\frac{\text{Joules}}{\text{kg } ^\circ\text{C}}\right)$
20	$.4182 \times 10^{4}$
75	$.3894 \times 10^{4}$
125	$.3652 \times 10^{4}$
200	$.3341 \times 10^{4}$

Density

for $T > 25^\circ C$

$$\rho(T) = 996.9 \cdot \left\{ 1 - 3.17 \times 10^{-4} \cdot (T-25) - 2.56 \times 10^{-6} \cdot (T-25)^2 \right\}$$

for $T < 25^\circ C$

$$\rho(T) = 996.9 \cdot \left\{ 1 - 1.87 \times 10^{-4} \ (T-25) \right\}$$

Table 4.

TEMPERATURES (^{o}C) FOR

DIFFERENT STORATIVITIES

Time	Radial Distance (m)	Storativity	
		5×10^{-4}*	1×10^{-2}**
End of Injection	10	54.79	54.79
1900 hours	20	54.97	54.97
	30	50.25	50.26
	40	27.94	27.95
End of Storage	10	54.76	54.76
3113 hours	20	54.93	54.93
	30	48.95	48.98
	40	28.54	28.57
End of Production	10	32.07	32.15
4100 hours	20	26.70	26.77
	30	21.92	21.95
	40	20.26	20.27

* Determined by well test analysis

** Used for CCC simulations

Table 5.

ENERGY BALANCE

First Cycle

INJ_1	= injected	$= .721 \times 10^{13}$ joules
$PROD_1$	= produced	$= .486 \times 10^{13}$
LEFT	= left in aquifer	$= .132 \times 10^{13}$
LOST	= lost from aquifer	$= .102 \times 10^{13}$

$\frac{PROD_1}{INJ_1} = .67$ $\frac{LEFT}{INJ_1} = .18$ $\frac{LOST}{INJ_1} = .14$

Second Cycle

INJ_2	= injected	$= .765 \times 10^{13}$
$PROD_2$	= produced	$= .591 \times 10^{13}$

$\frac{PROD_2}{INJ_2} = .77$

Cumulative

INJ	$= INJ_1 + INJ_2$	$= .149 \times 10^{14}$
PROD	$= PROD_1 + PROD_2$	$= .108 \times 10^{14}$
LEFT	= left in aquifer	$= .198 \times 10^{13}$
LOST	= lost from aquifer	$= .211 \times 10^{13}$

$\frac{PROD}{INJ} = .72$ $\frac{LEFT}{INJ} = .13$ $\frac{LOST}{INJ} = .14$

Figure Captions

Figure 1 shows the well field layout. I is the injection/production well.

Figure 2 shows a cross section of the radially symmetric mesh used in the simulation. The shaded elements represent the injection/production well.

Figure 3 shows the experimental injection flowrate and temperatures versus time, and the average values used in the simulation.

Figure 4 shows the simulated temperature contours in a vertical cross-section of the aquifer after 287 hours of injection. The shaded area represents the screened portion of the injection/production well. The horizontal lines at 18.8 and 40 meters depth mark the upper and lower boundaries of the aquifer.

Figure 5 shows the simulated temperature contours, as well as the observed temperatures at the end of the first cycle injection, 1900 hours. Note that the observation wells do not lie along one radius, but are distributed as shown in Figure 1.

Figures 6-9 show the simulated and observed temperatures at mid-aquifer depth for each observation well during the injection period. Notice figure 9 which shows wells 4 and 8. Although they are at about the same distance from the well, they lie in opposite directions. The barrier boundary to the Northwest of the well field noted in the well test analyses would cause just the temperature variation between wells 4 and 8 that is noted.

Figures 10-12 show the temperature distribution at various depths in the aquifer, at the end of the injection period. The injection/production well is at 0-2 meters radial distance. Figure 10 shows the simulated temperature from the nodes that lie above and below the depth at which the observed temperature was measured.

Figures 13 and 14 show the simulated temperature contours, as well as the observed temperatures at the end of the first cycle storage, 3113 hours, and the end of the first cycle production, 4100 hours. The location of the injection/production well is marked by the straight line segments at r = 0-2 meters.

Figure 15 shows the observed and simulated first cycle production temperatures as a function of time.

Figure 16 compares the 1900 hour temperature distributions simulated using the coarse, medium, and fine meshes. Note that at depths of 13 and 17 meters the medium and fine meshes yield identical results.

Figure 17 compares the production temperature versus time for the coarse and medium meshes.

Figures 18 and 19 show the simulated temperature contours, as well as the observed temperatures at the end of the second cycle injection, 1521 hours, and the end of the second cycle production, 4351 hours.

Figure 20 shows the observed and simulated second cycle production temperature as a function of time. The arrow marks the time through which the energy recovery factor was calculated.

Figure 1.

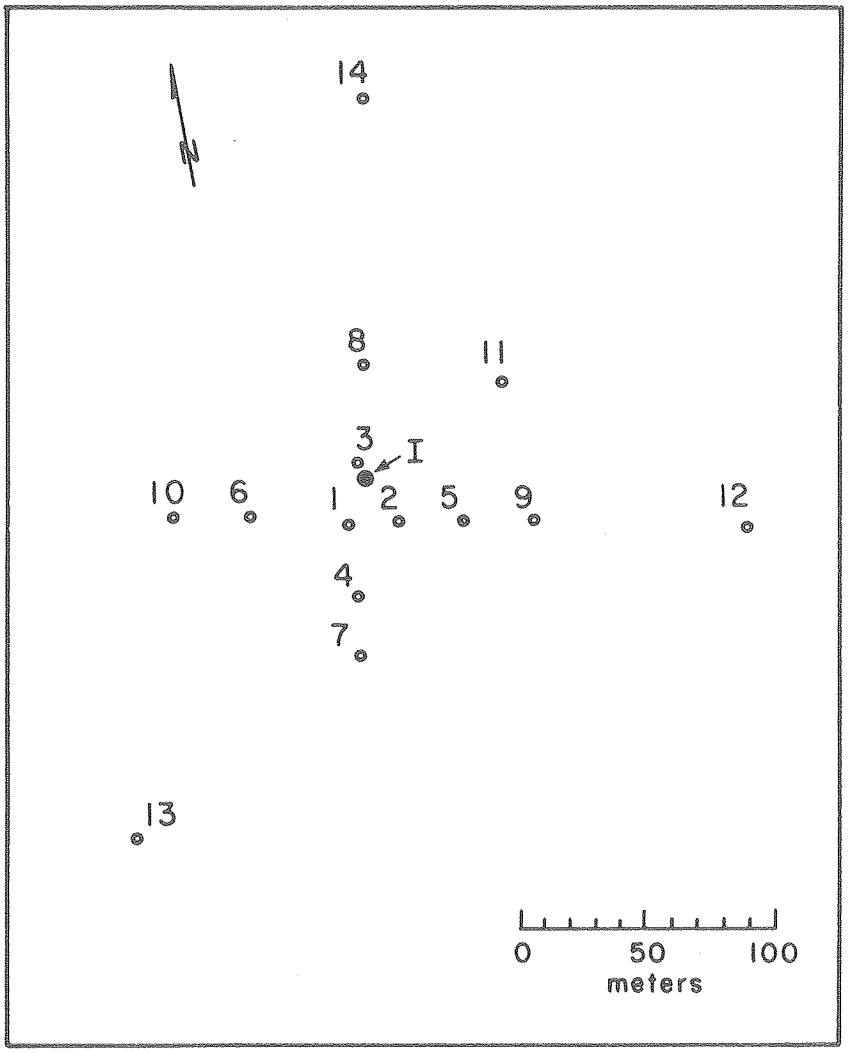

XBL 795-7445A

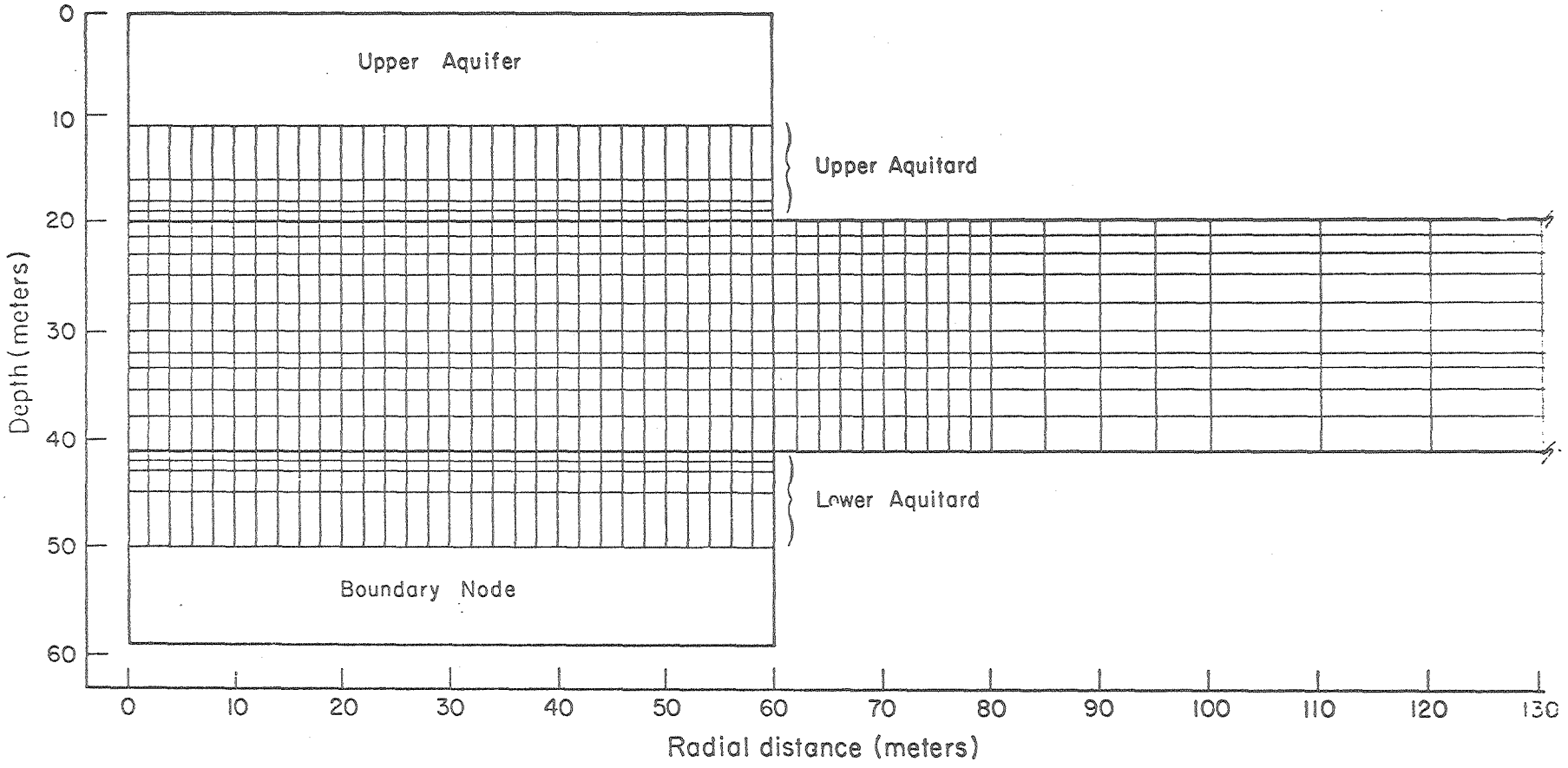
Cross section of radial mesh
Upper Aquifer
Upper Aquitard
Lower Aquitard
Boundary Node
Depth (meters)
0
10
20
30
40
50
60
0
10
20
30
40
50
60
70
80
90
100
110
120
130
Radial distance (meters)
XBL 795-7453

Figure 2.

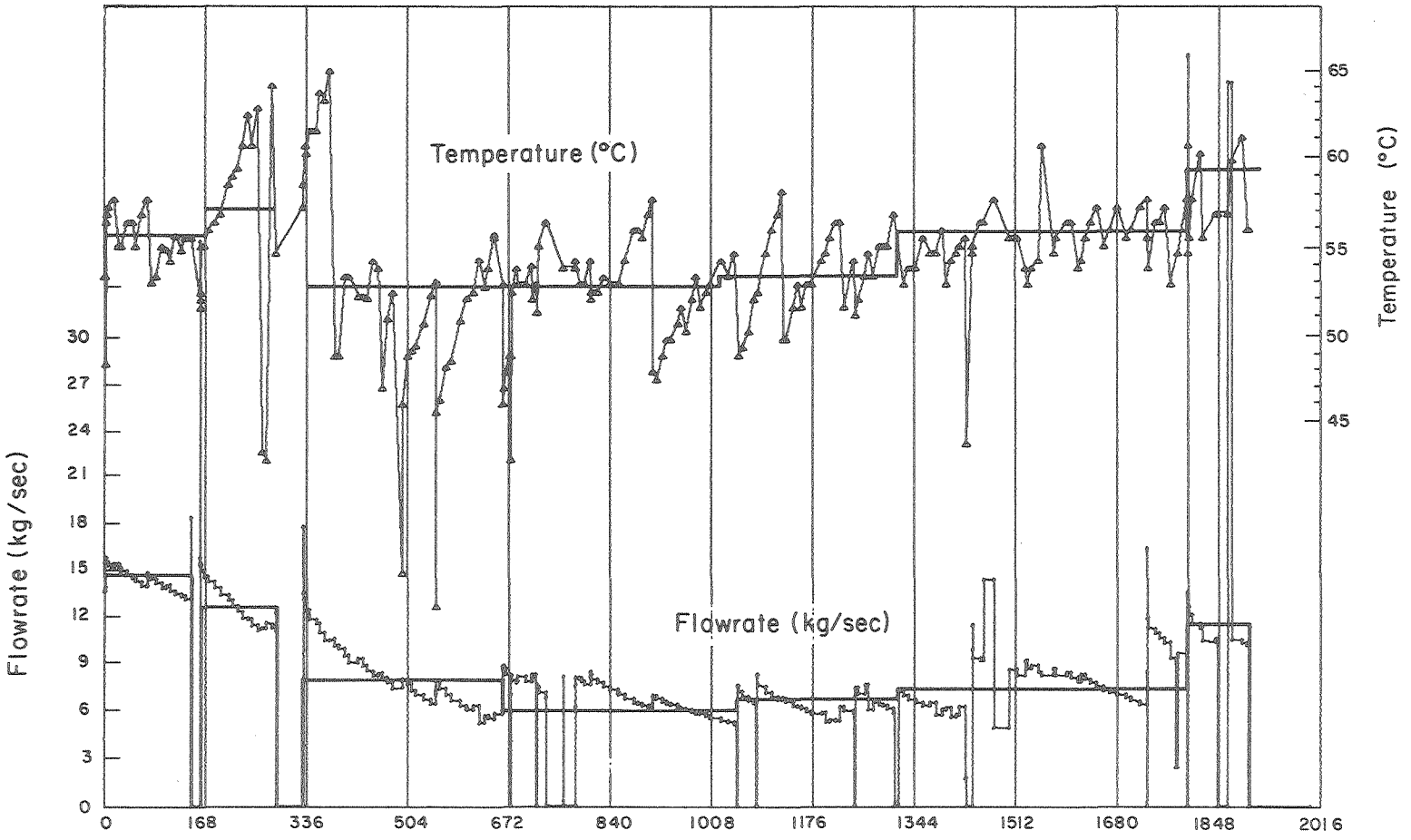

AUBURN INJECTION FLOWRATE AND TEMPERATURE
FIRST CYCLE

XBL 795-7460

Figure 3.

Figure 4.

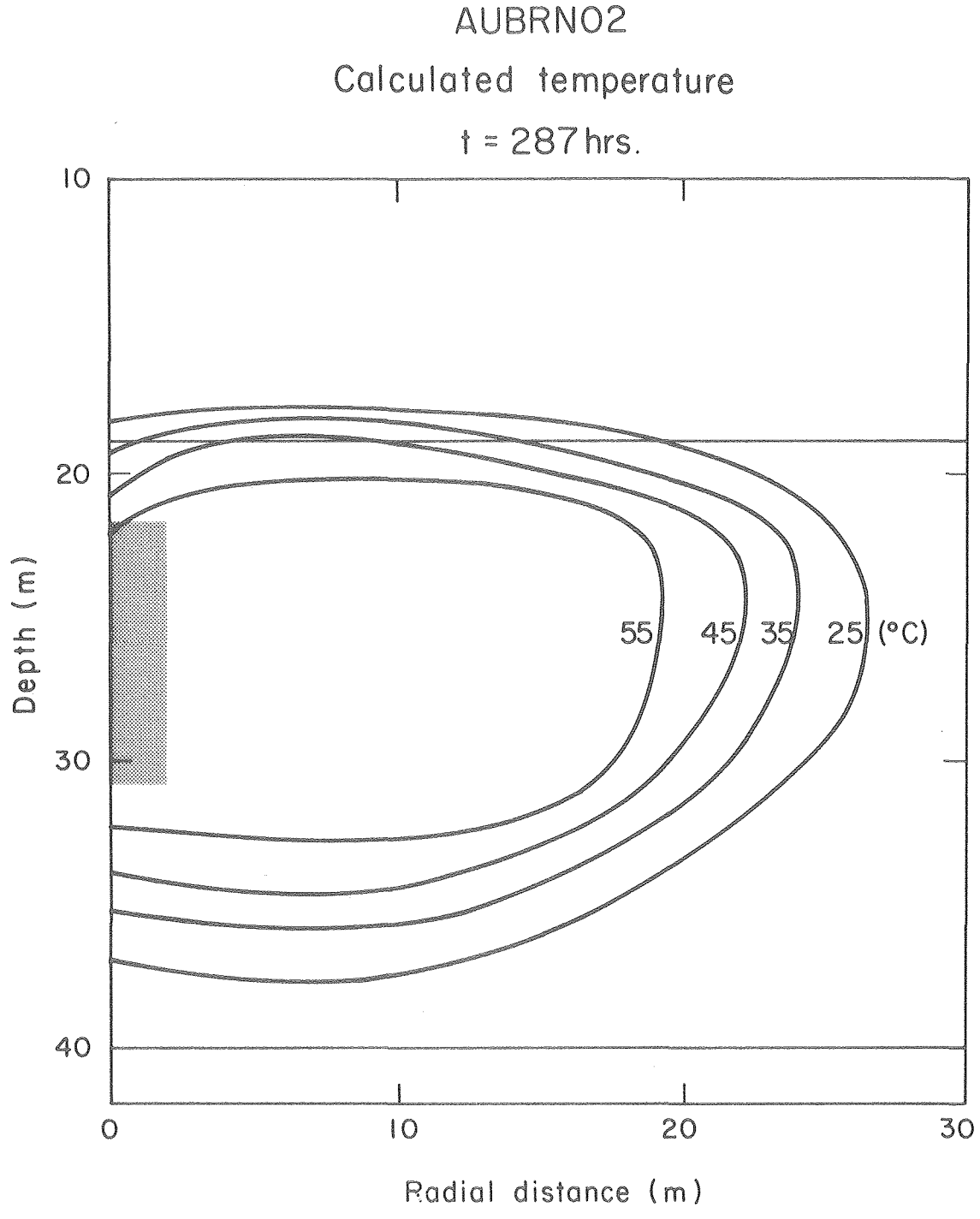

XBL 795-7449

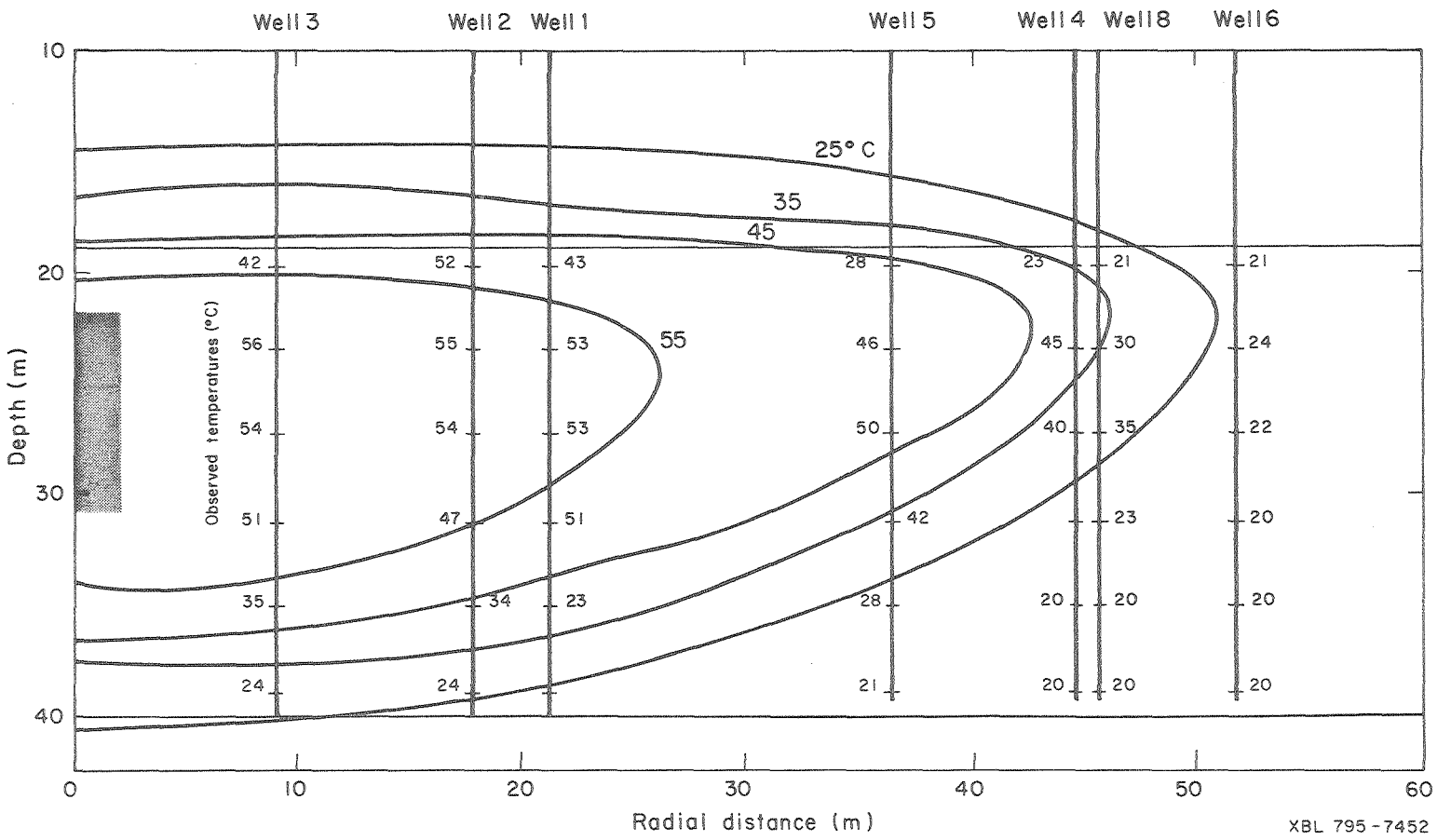
AUBRNO 2
Calculated temperature
t = 1900 hrs.
Well 3
Well 2
Well 1
Well 5
Well 4
Well 8
Well 6
25° C
35
45
55
Observed temperatures (°C)
42
52
43
28
23
21
21
56
55
53
46
45
30
24
54
54
53
50
40
35
22
51
47
51
42
23
20
35
34
23
28
20
20
20
24
24
21
20
20
20
Depth (m)
10
20
30
40
0
10
20
30
40
50
60
Radial distance (m)
XBL 795-7452

Figure 5.

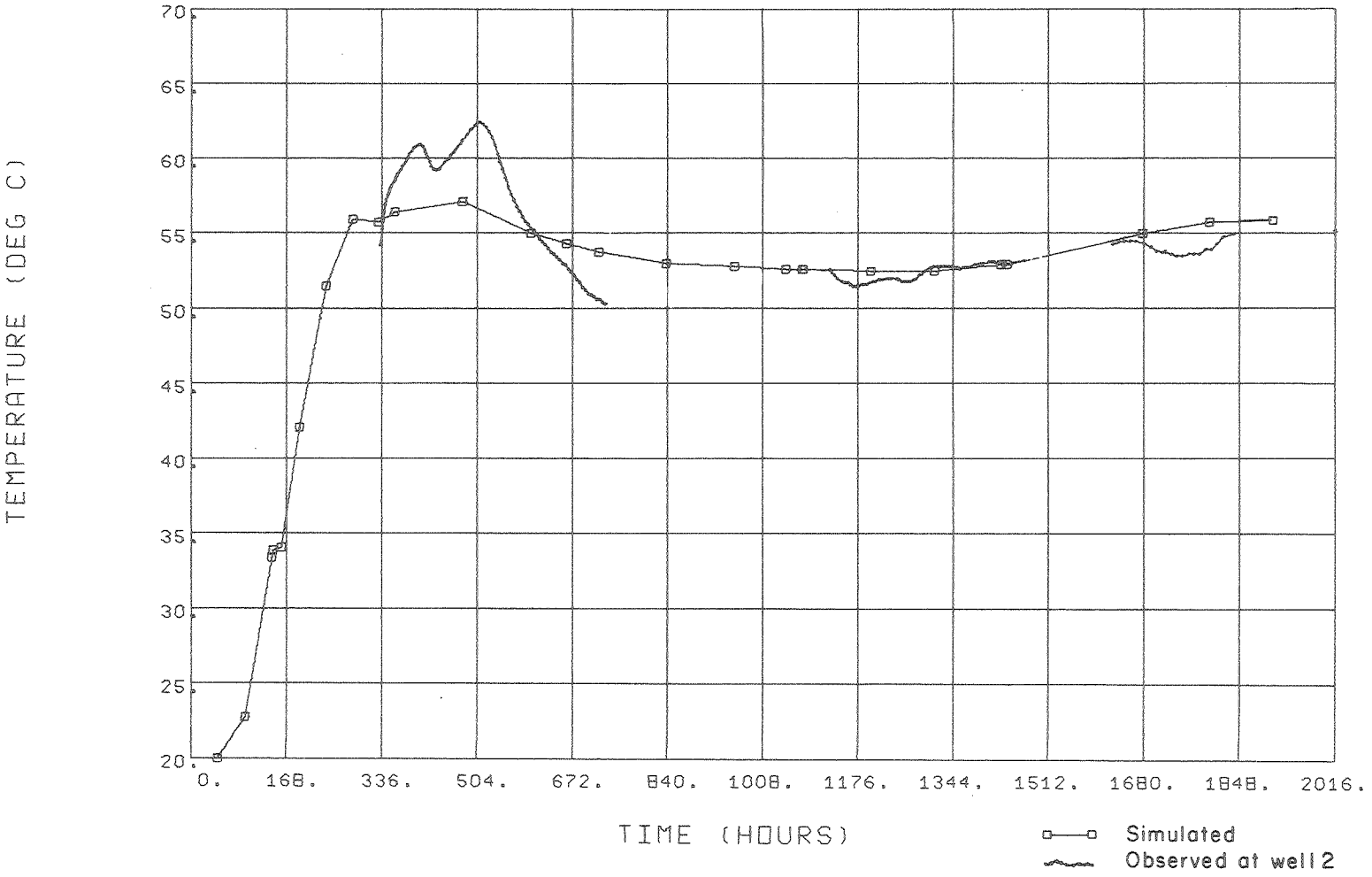

AUBURN TEMPERATURE AT 18 METERS

XBL 795-7454

Figure 6.

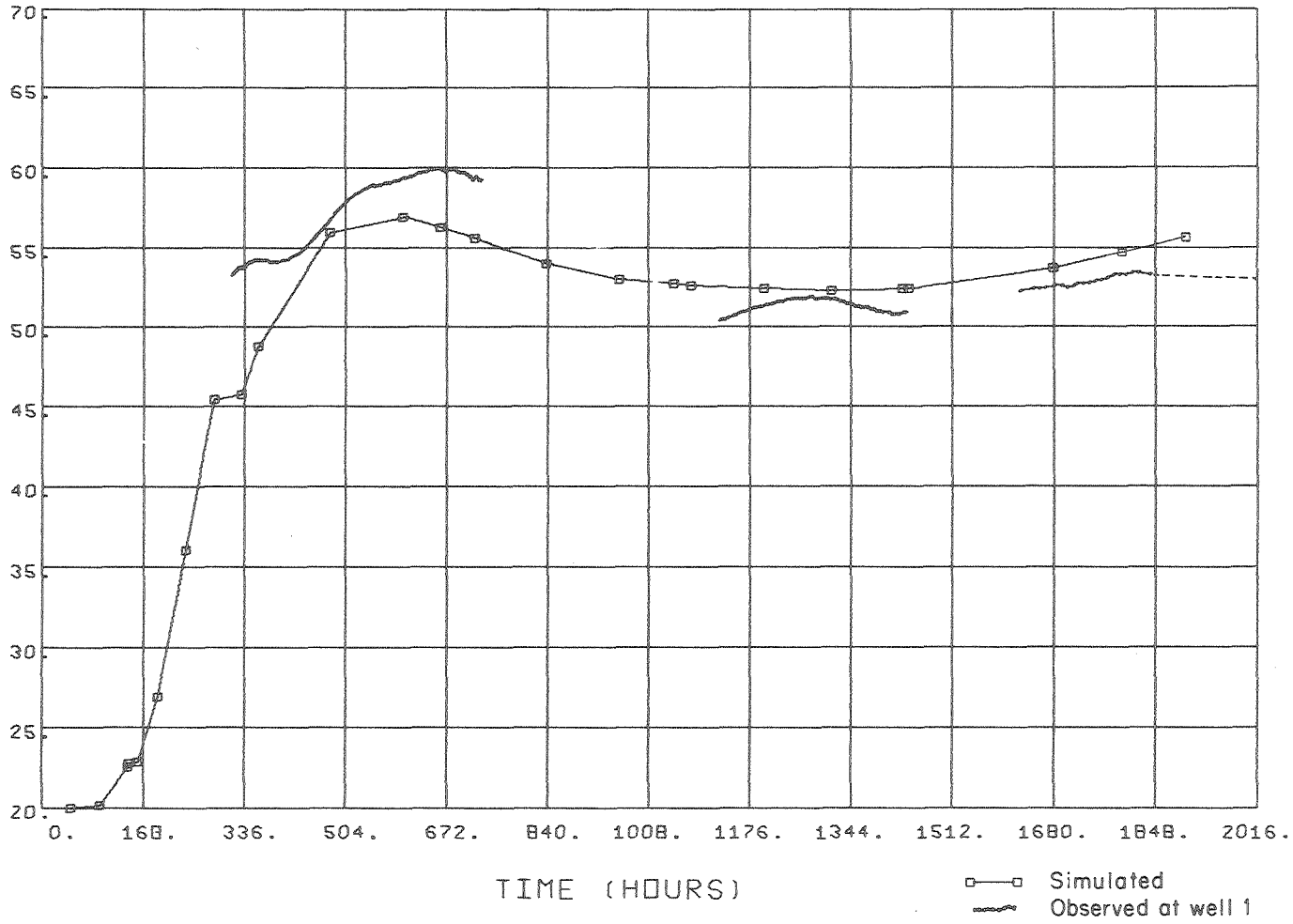

AUBURN TEMPERATURE AT 21 METERS

XBL 795-7456

Figure 7.

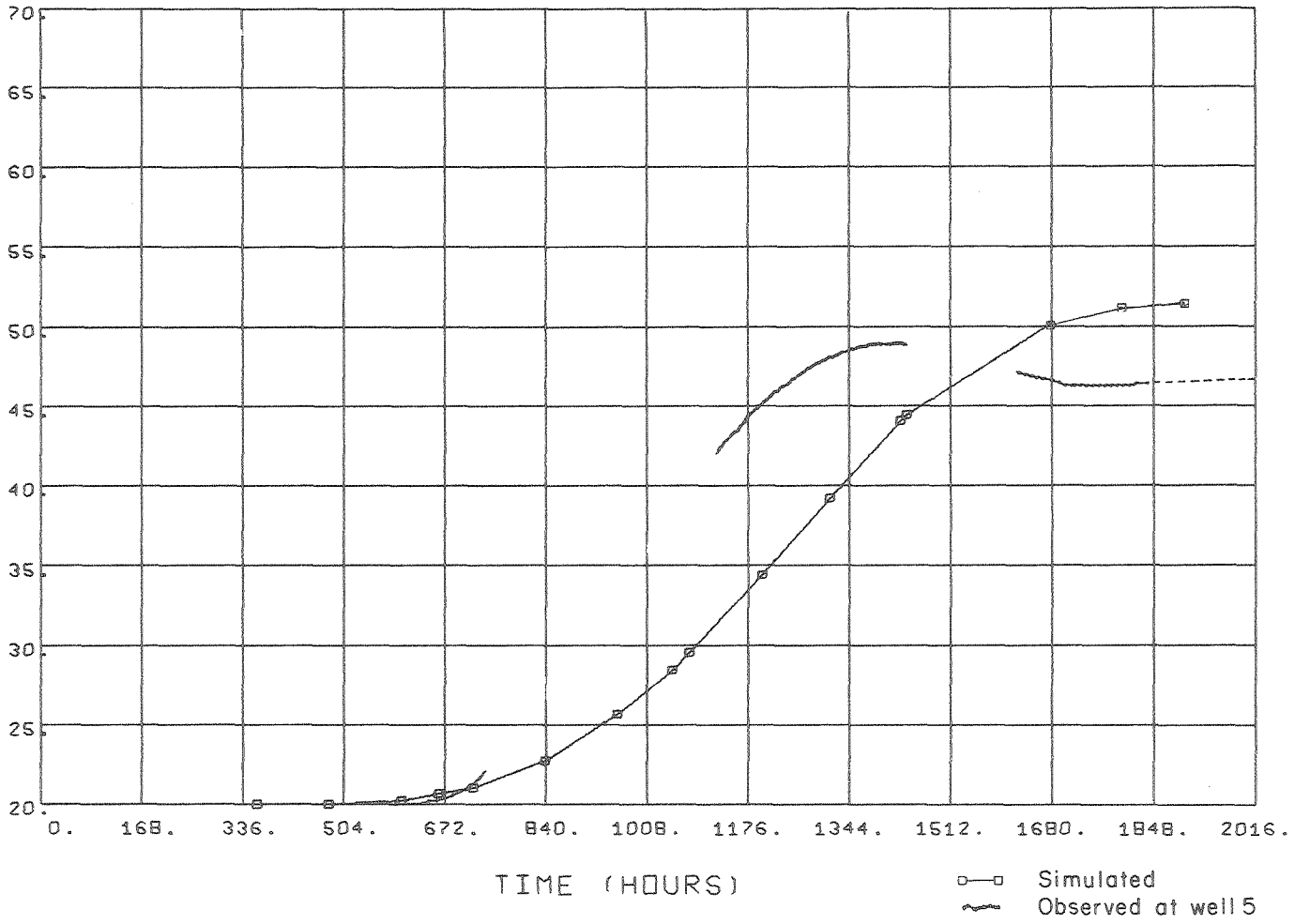

AUBURN TEMPERATURE AT 37 METERS

XBL 795-7457

Figure 8.

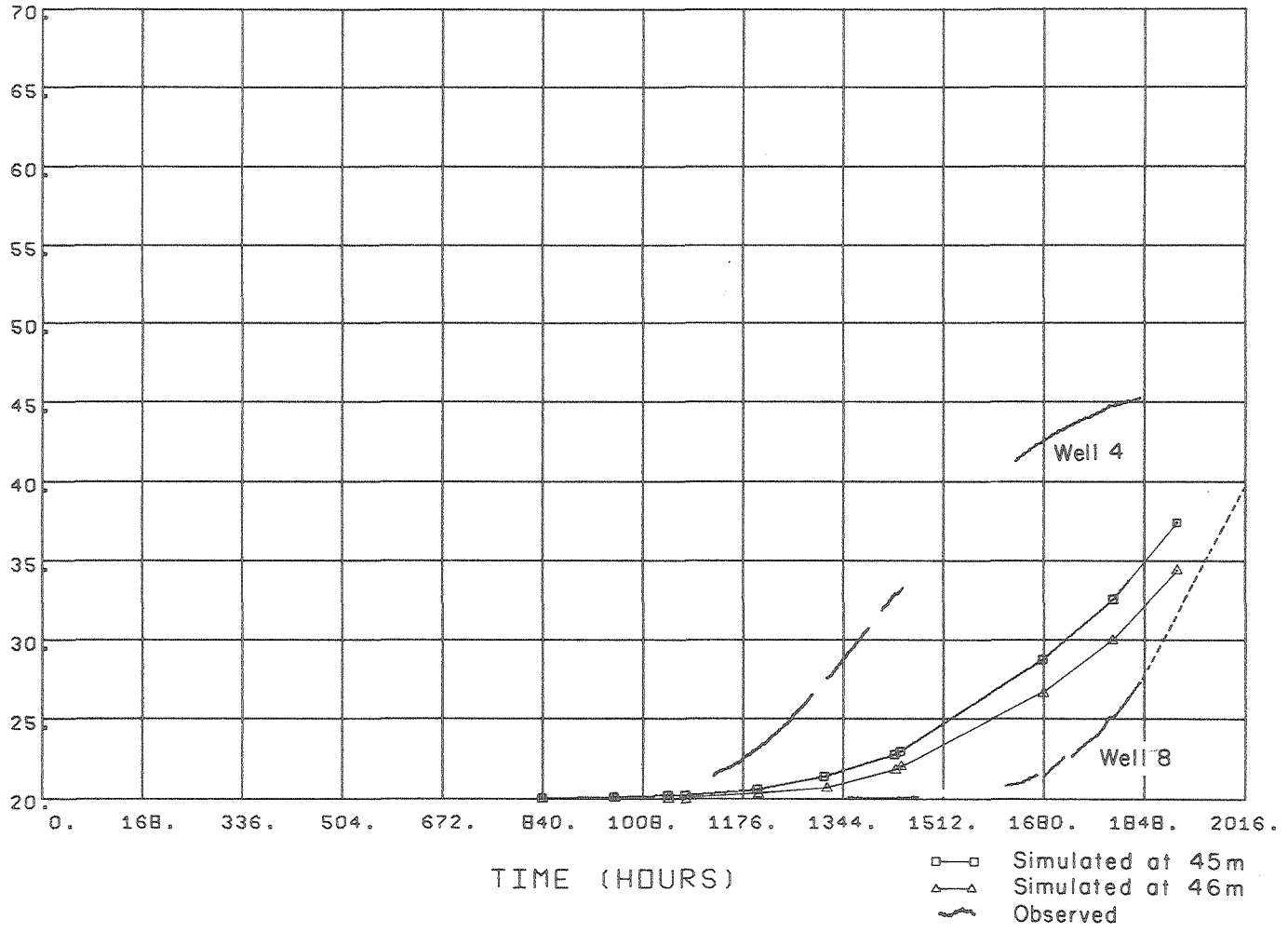

AUBURN TEMPERATURE AT 45 and 46 METERS

XBL 795-7459

Figure 9.

Figure 10.

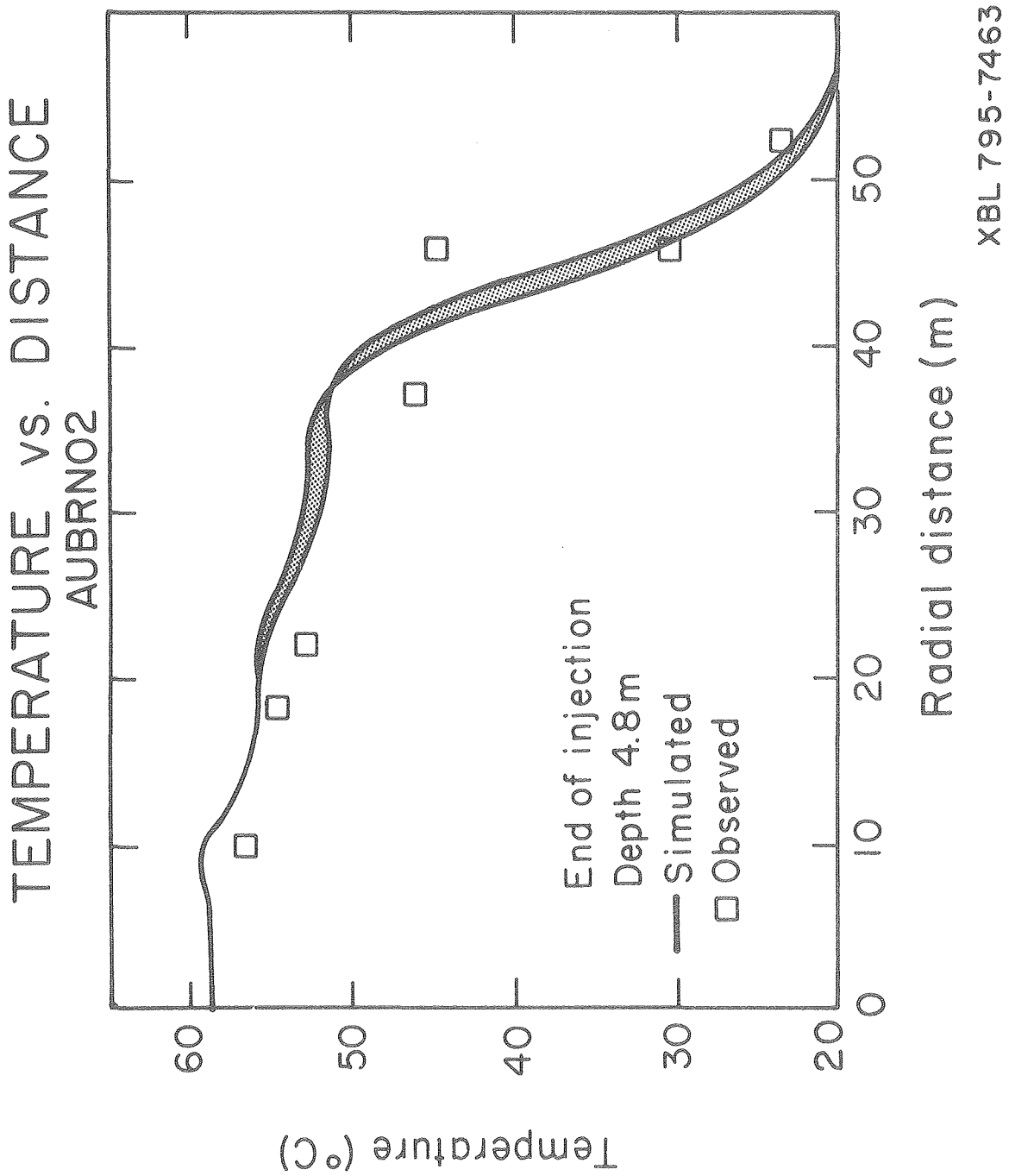
TEMPERATURE vs. DISTANCE
AUBRN02
End of injection
Depth 4.8m
Simulated
Observed
Temperature (°C)
Radial distance (m)
XBL 795-7463

Figure 11.

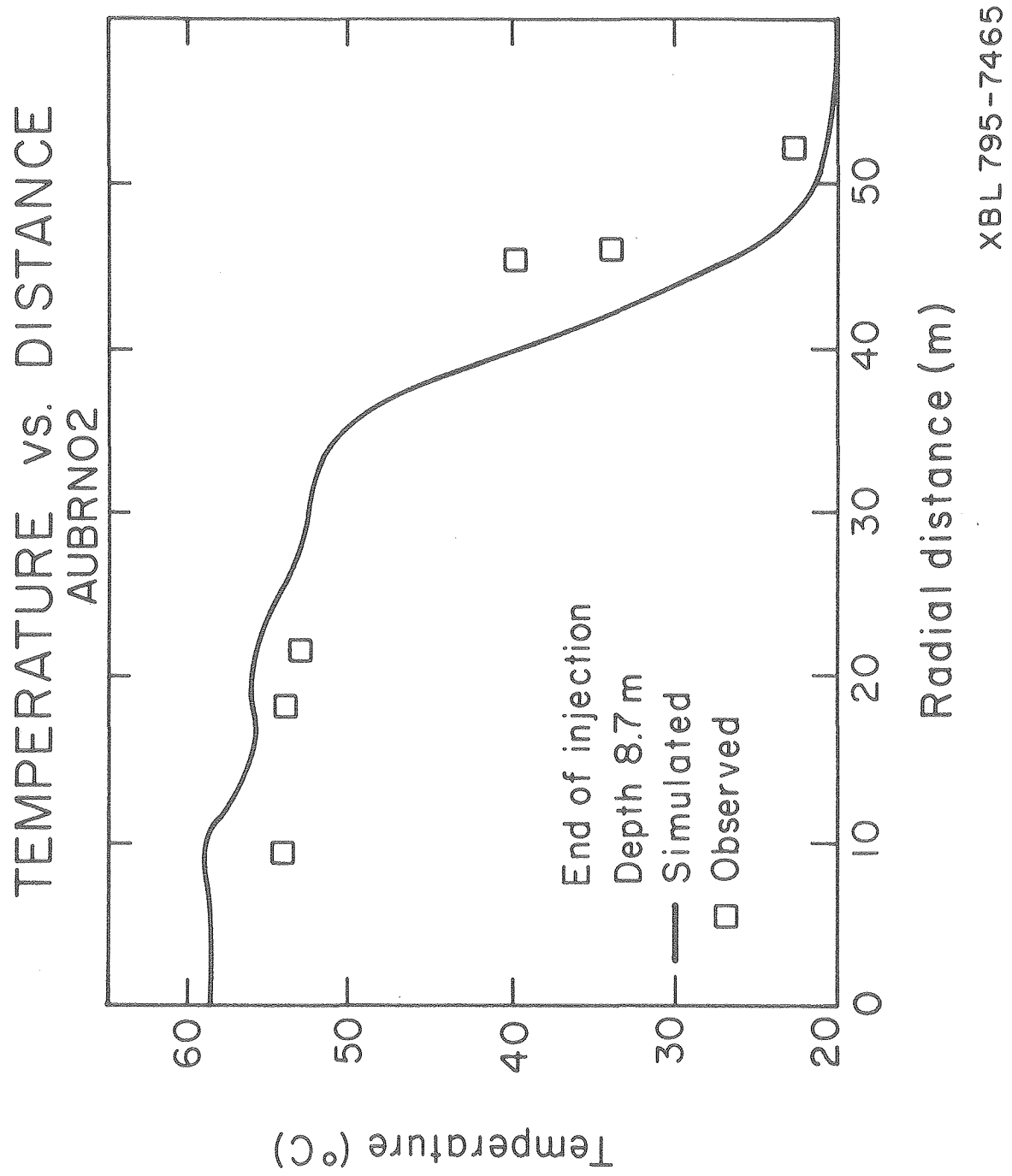
TEMPERATURE vs. DISTANCE
AUBRN02
Temperature (°C)
60
50
40
30
20
0
10
20
30
40
50
Radial distance (m)
End of injection
Depth 8.7 m
Simulated
Observed
XBL 795-7465

Figure 12.

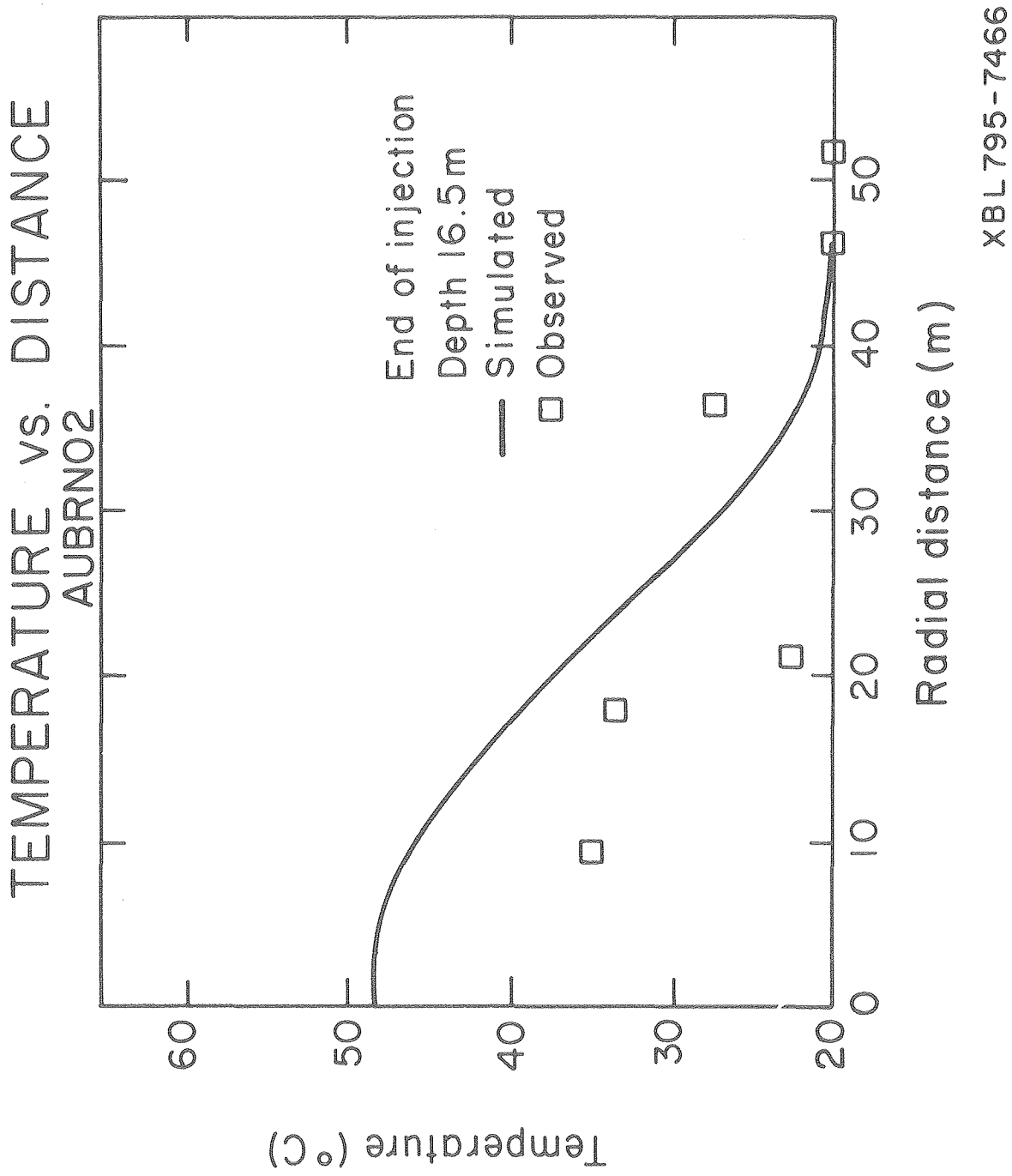
TEMPERATURE vs. DISTANCE
AUBRN02
End of injection
Depth 16.5m
Simulated
Observed
Temperature (°C)
Radial distance (m)
XBL795-7466

CALCULATED TEMPERATURE CONTOURS

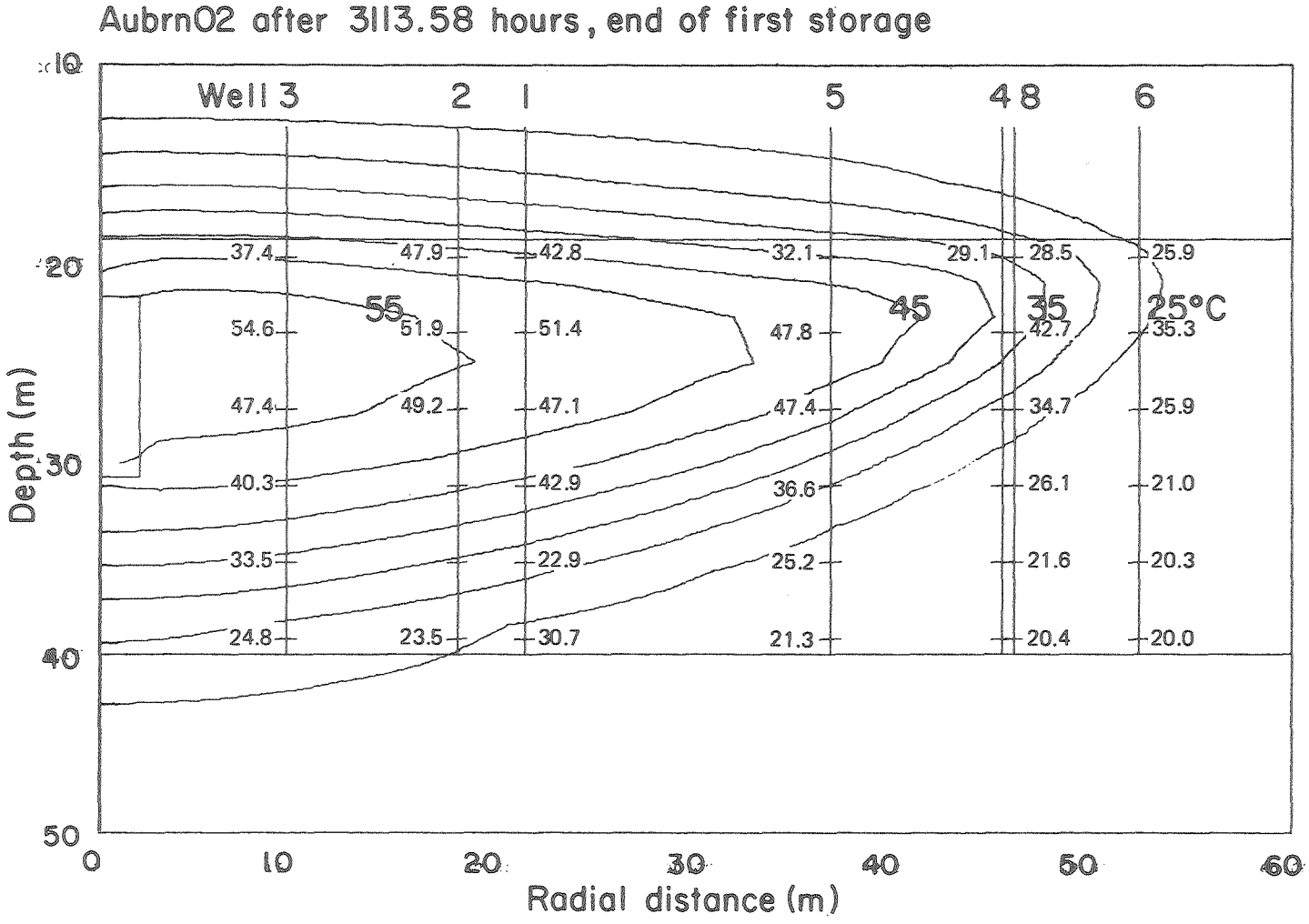

XBL 798-11434A

Figure 13.

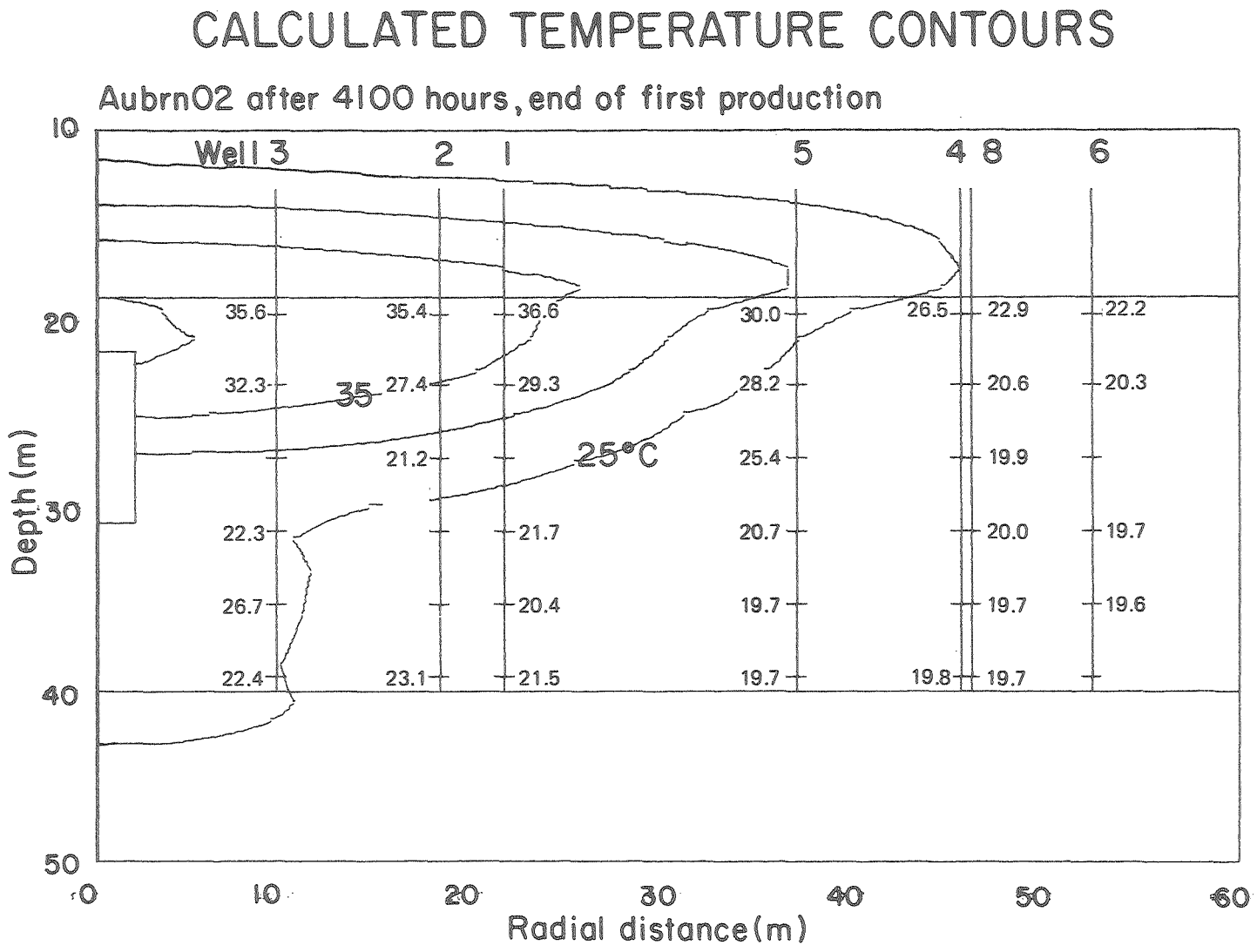

XBL 798-11435A

Figure 14.

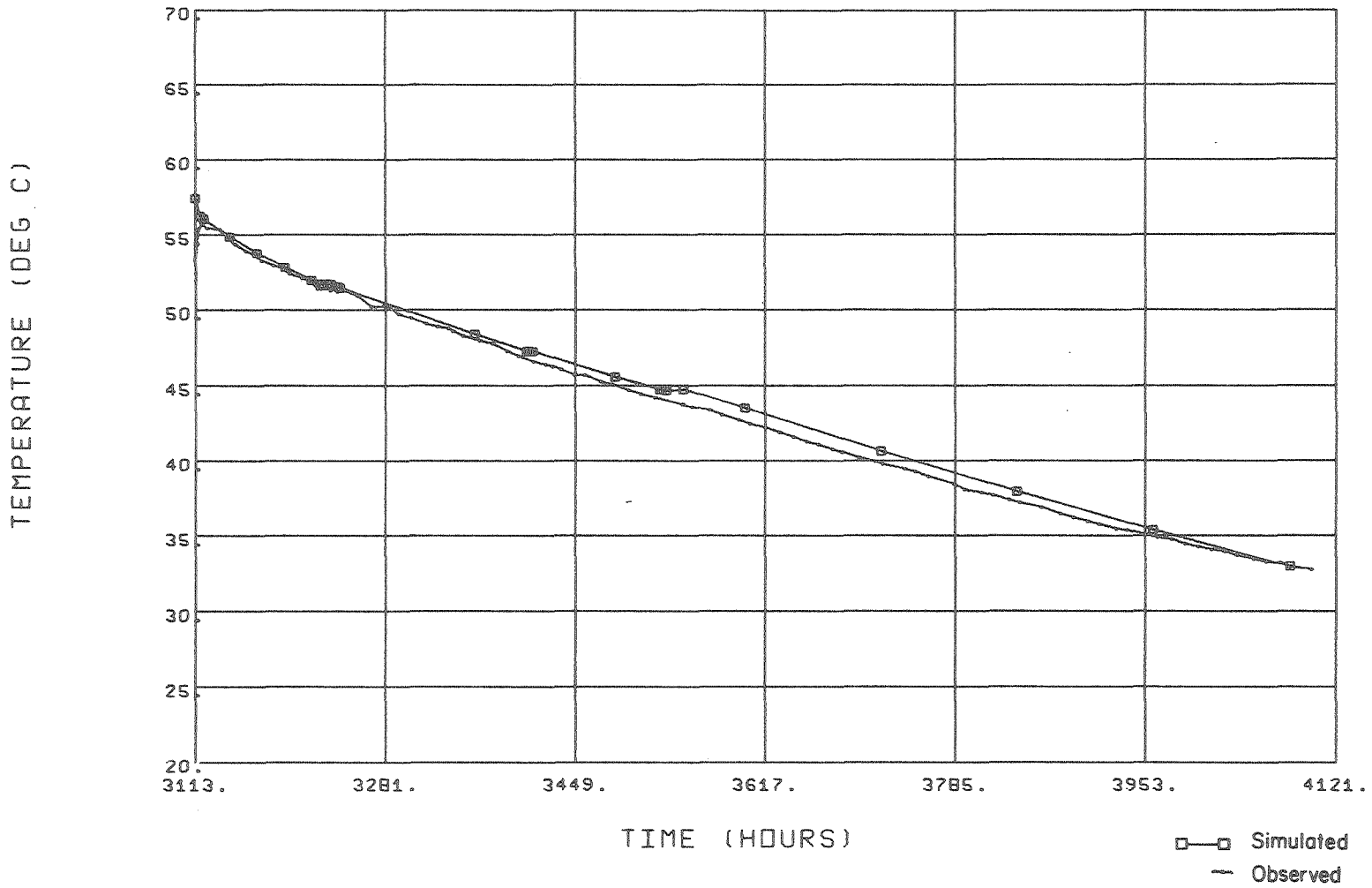

AUBURN PRODUCTION TEMPERATURE
FIRST CYCLE

XBL 798-11428

Figure 15.

Figure 16.

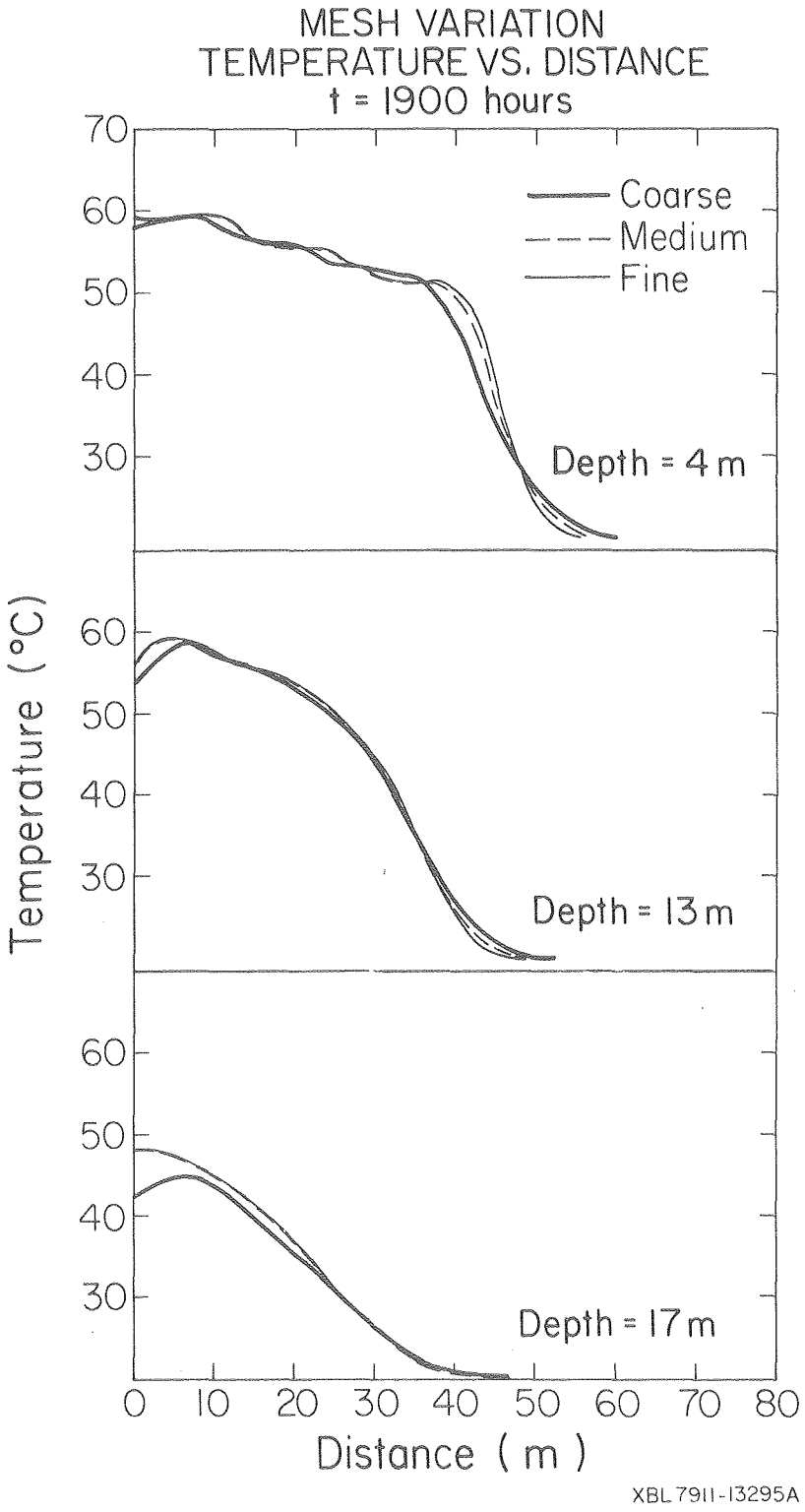
MESH VARIATION
TEMPERATURE VS. DISTANCE
t = 1900 hours
Coarse
Medium
Fine
Depth = 4 m
Depth = 13 m
Depth = 17 m
Temperature (°C)
70
60
50
40
30
0
10
20
30
40
50
60
70
80
Distance (m)
XBL 7911-13295A

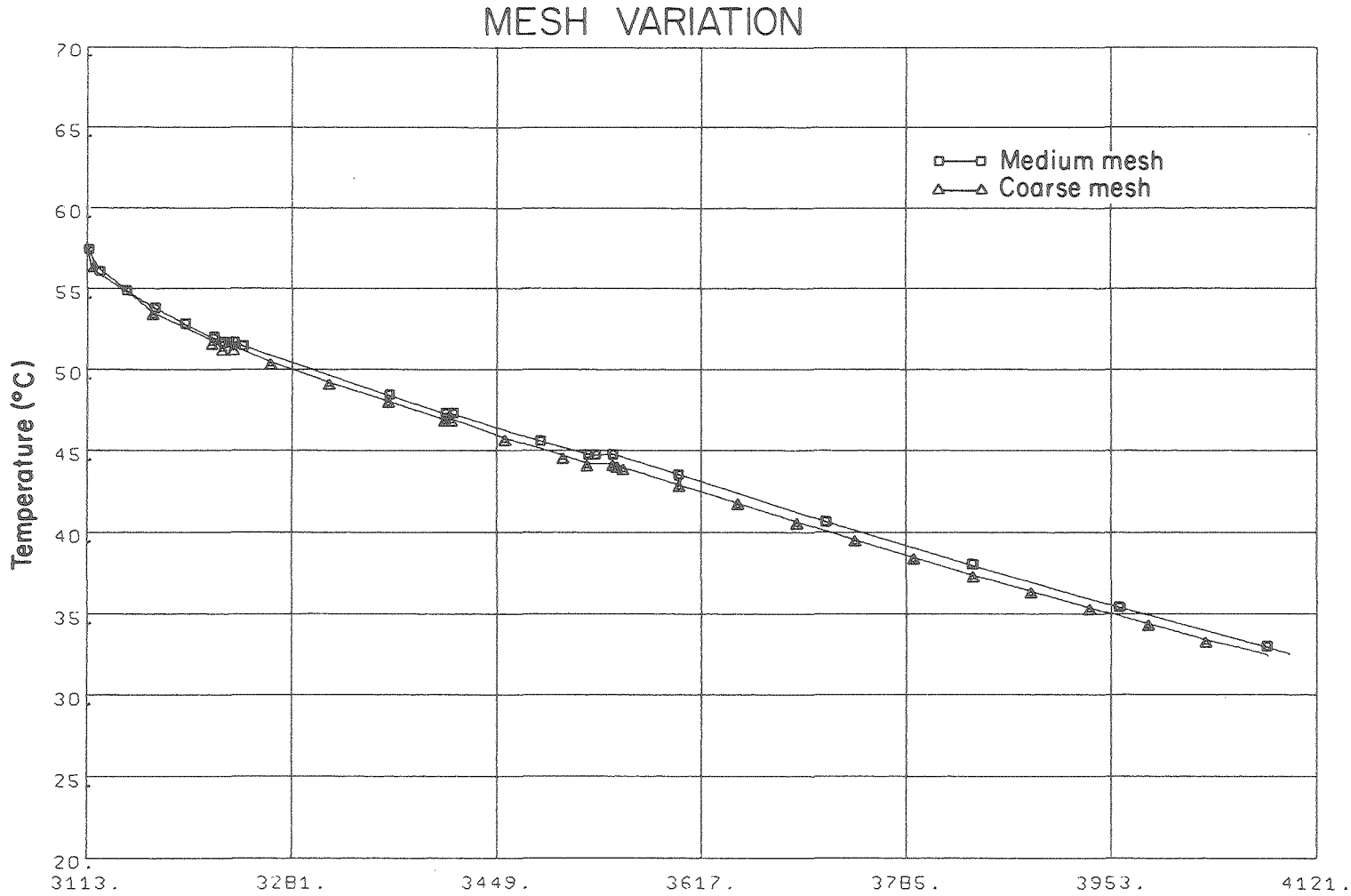

AUBURN PRODUCTION TEMPERATURE

XBL 7912-13756

Figure 17.

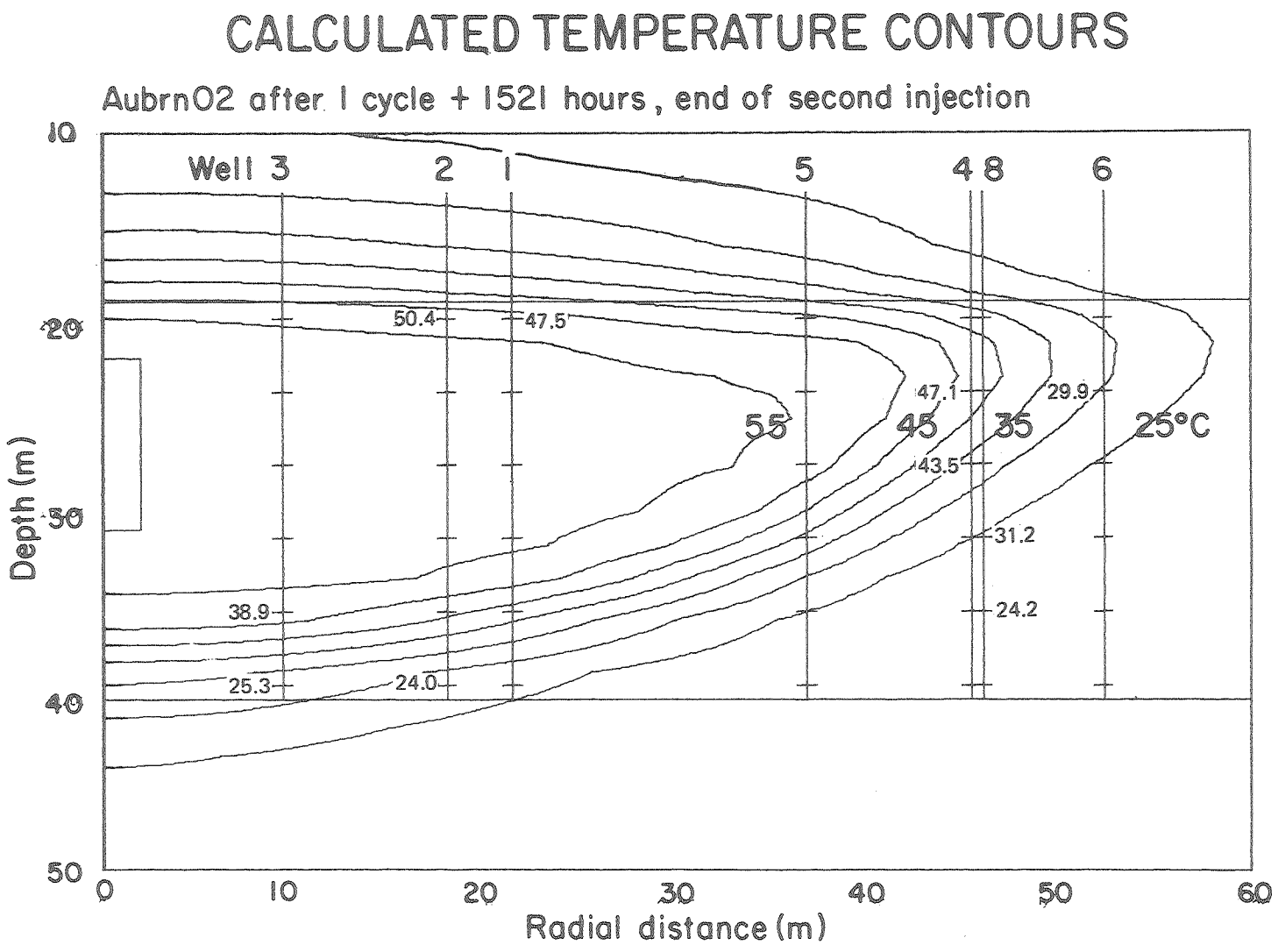

XBL 798-11436A

Figure 18.

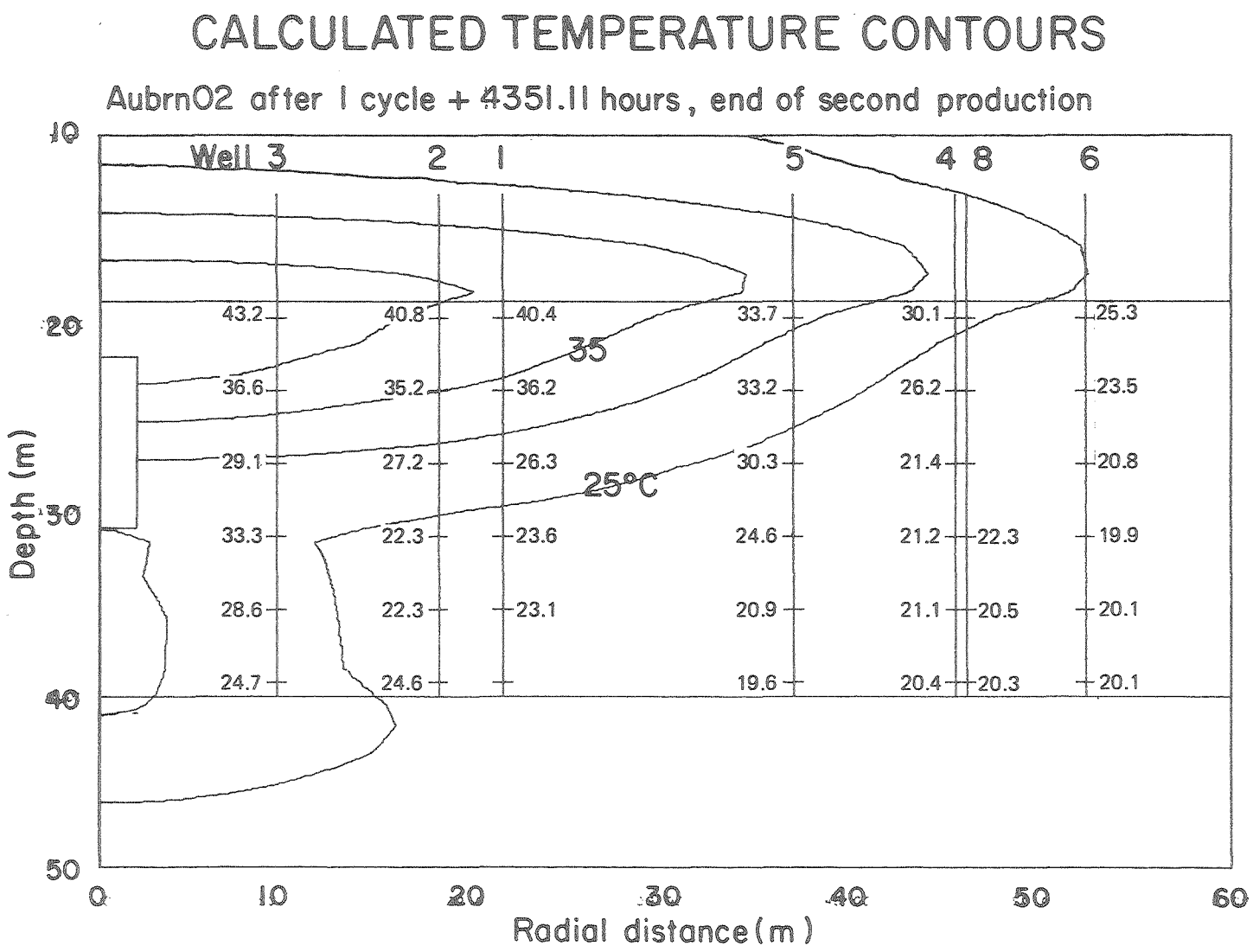

XBL 798-11438A

Figure 19.

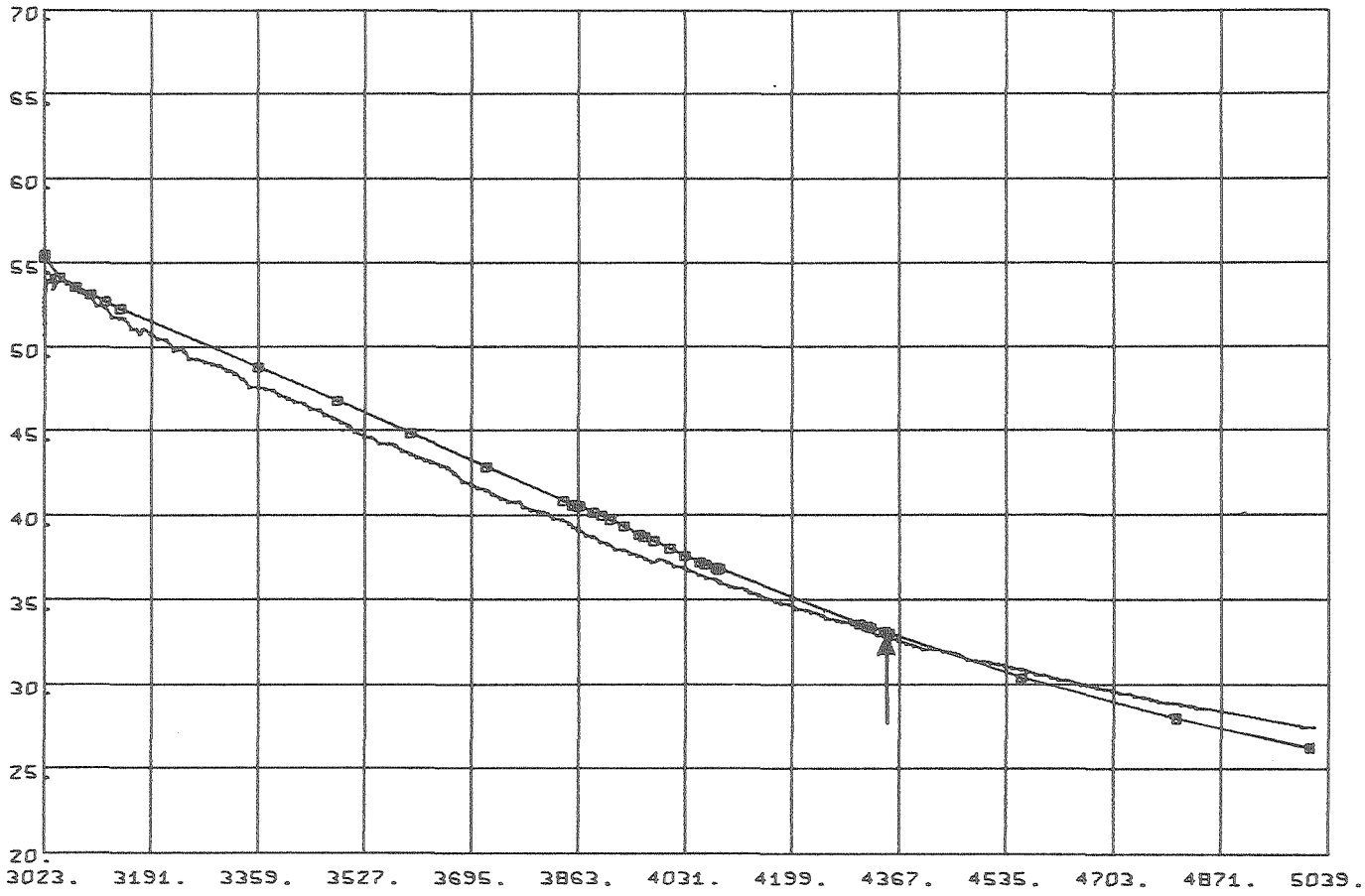

AUBURN PRODUCTION TEMPERATURE
SECOND CYCLE

XBL 798-11426

Figure 20.